faces of HIV-1-producing $CD4^+$ T cells and colocalize with HIV-1 Env and Gag (35).

Recently, it was suggested that CD63 plays roles in HIV-1 replication. For example, Lindern et al. reported that the pretreatment of macrophages with anti-CD63 antibodies inhibits HIV-1 infection (70). In addition, Ho et al. have shown that the recombinant soluble protein of the large extracellular loop (LEL) of CD63 potently inhibits HIV-1 infection to macrophages, presumably at the entry step (33). Nevertheless, the practical role(s) and function(s) of intact CD63 protein in HIV-1 infection are still unclear.

Here, we investigated whether CD63 has any virological function in HIV-1 infection. We observed that CD63 was removed from the plasma membrane of HIV-1-producing T cells by activation stimuli, and that the activated cells released HIV-1 virions that contained smaller amounts of CD63 and had higher infectivity. In addition, through exogenous expression experiments, we found evidence suggesting that CD63 at the plasma membrane of HIV-1-producing cells was efficiently incorporated into released virions and that virion-incorporated CD63 had the potential to impair HIV-1 Env-mediated infection in a strain-specific manner at the postattachment step(s). Similar behavior was also observed in other tetraspanin proteins, such as CD9, CD81, CD82, and CD231. However, L6, which has topology similar to that of tetraspanins but does not belong to the tetraspanin superfamily, did not have the potential to prevent HIV-1 infection. These are the first findings suggesting that some cellular membrane proteins can attenuate HIV-1 Env-mediated infection in a strain-specific manner through incorporation into released HIV-1 particles.

MATERIALS AND METHODS

Cells. 293T cells and MAGIC-5 cells (HeLa cells transduced with genes for CD4, CCR5, and long terminal repeat-driving β-galactosidase) (29) were maintained in Dulbecco's modified Eagle medium containing 10% fetal calf serum (FCS), 100 U/ml penicillin, and 100 μg/ml streptomycin. Molt4/IIIB cells, which persistently produce $HIV\text{-}1_{IIIB}$ (39), and MT-4 cells were maintained in RPMI 1640 medium containing 10% FCS, 100 U/ml penicillin, and 100 μg/ml streptomycin. To activate Molt4/IIIB cells, 1 μg/ml phytohemagglutinin (PHA) and 100 ng/ml phorbol 12-myristate 13-acetate (PMA) were added, and cells were cultured for 72 h. To prepare activated primary $CD4^+$ T cells, peripheral blood mononuclear cells (PBMCs) were isolated from peripheral blood of healthy HIV-1-seronegative donors as previously described (41). $CD4^+$ T cells were isolated from the PBMCs by using a CD4-positive-cell isolation kit (Dynal, Oslo, Norway) and were activated by using a Dynabeads CD3/CD28 T-cell expander (Dynal) according to the manufacturer's instructions. Activated primary $CD4^+$ T cells were maintained in RPMI 1640 containing 10% FCS, 100 U/ml interleukin-2 (Shionogi, Osaka, Japan), 100 U/ml penicillin, and 100 μg/ml streptomycin.

Plasmid construction. To construct a CD63 expression plasmid (pCD63), a *cd63* cDNA fragment was amplified by PCR from a human leukocyte cDNA library (Invitrogen, Carlsbad, CA) using the following primers: sense, 5′-TA GCG AAT TCC ATG GCG GTG GAA GGA G-3′; antisense, 5′-TA GCT CTA GAC CTA CAT CAC CTC GTA GCC ACT-3′. The resulting fragment was digested with EcoRI and XbaI and inserted into the EcoRI-XbaI site of pCMV-SPORT6 (Invitrogen). To construct CD9-, CD81-, CD82-, and CD231-expressing plasmids (pCD9, pCD81, pCD82, and pCD231), *cd9*, *cd81*, *cd82*, and *cd231* cDNA fragments were obtained similarly, using the following primers: *cd9* sense, 5′-TT TTG AAT TCC ATG CCG GTC AAA GGA GGC A-3′; *cd9* antisense, 5′-TT TTT GAT ATC CTA GAC CAT CTC GCG GTT CCT-3′; *cd81* sense, 5′-TT TTG AAT TCC ATG GGA GTG GAG GGC TGC A-3′; *cd81* antisense, 5′-TT TTT GAT ATC TCA GTA CAC GGA GCT GTT CCG GAT-3′; *cd82* sense, 5′-TT TTG AAT TCC ATG GGC TCA GCC TGT ATC AAA G-3′; *cd82* antisense, 5′-TT TTT GAT ATC TCA GTA CTT GGG GAC CTT GCT GT A-3′; *cd231* sense, 5′-TT TTG GTA CCC ATG GCA TCG AGG AGA ATG GA-3′; *cd231* antisense, 5′-TT TTT GAT ATC TTA CAC CAT CTC ATA CTG ATT GGC-3′. The *cd9* cDNA fragment was also amplified from the leukocyte library, whereas *cd81*, *cd82*, and *cd231* cDNA fragments were obtained by reverse transcription-PCR of mRNA derived from Jurkat cells. These cDNA fragments were digested with EcoRI and EcoRV and inserted into the EcoRI-EcoRV site of pCMV-SPORT6. To construct an L6-expressing plasmid (pL6), *l6* cDNA was obtained from pRcCMV-L6 (kindly provided by E. Mekada) using the following primers: *l6* sense, 5′-TT TTG GTA CCC ATG TGC TAT GGG AAG TGT GCA-3′; *l6* antisense, 5′-TT TTT GAT ATC TTA GCA GTC ATA TTG CTG TTG GTG-3′. The resulting fragment was digested with KpnI and EcoRI and inserted into the KpnI-EcoRI site of pCMV-SPORT6. To construct pCD63ΔL, expressing a CD63 with the lysosomal sorting motif deleted (CD63ΔL), pCD63 was digested with PstI and XbaI, and the following mutagenic oligonucleotides were inserted: sense, 5′-GCA GCC CTT GGA ATT GCT TTT GTC GAG GTT TTG GGA ATT GTC TTT GCC TGC TGC CTC GTG AAG AGT ATC AGA TAG T-3′; antisense, 5′-CT AGA CTA TCT GAT ACT CTT CAC GAG GCA GCA GGC AAA GAC AAT TCC CAA AAC CTC GAC AAA AGC AAT TCC AAG GGC TGC TGC A-3′. To construct pJRFLenv, a HindIII-XhoI fragment containing $HIV\text{-}1_{JR\text{-}FL}$ *tat*, *rev*, and *env* was inserted into pGEM4 (Promega, Madison, WI). To construct pNL4-3Δenv (which lacks $HIV\text{-}1_{NL4\text{-}3}$ *env*), pNL4-3 was digested with NheI, blunted, and self-ligated. PCR was carried out with the Expand Long Template PCR system (Roche, Mannheim, Germany), and reverse transcription-PCR was carried out by using SuperScript One-Step RT-PCR with Platinum high-fidelity *Taq* (Invitrogen), according to the manufacturer's protocols. Sequences of these plasmid constructs were confirmed with an ABI Prism 3100 genetic analyzer (Applied Biosystems, Foster City, CA).

Virus preparation. 293T cells were seeded to appropriate densities 1 day prior to transfection and were transfected by the calcium phosphate method as described previously (36). The culture supernatants were harvested, centrifuged, and then filtrated to produce virus solutions at 48 h posttransfection. To prepare HIV-1 and virus-like particles (VLPs), cells were cotransfected with pNL4-3 (1), pJR-FL (40), pNLFLV3 (kindly provided by W. A. O'Brien) (63), pNL4-3Δenv, and either tetraspanin-expressing plasmids or pCMV-SPORT6 (empty vector). To prepare pseudotyped viruses with envelope protein (Env) from either HIV-1 (NL4-3, IIIB, JR-FL, and NL4-3ΔCT, which encodes an NL4-3 Env with a deletion of the cytoplasmic tail [CT]) or vesicular stomatitis virus (VSV), cells were cotransfected with the Env expression plasmid DNA, pIIINL4env (kindly donated by T. Murakami and E. O. Freed) (48), pLET (59), pJRFLenv, pIIINL4envCTdel-144-2 (kindly donated by T. Murakami and E. O. Freed) (48), or pMD.G (53), respectively, and with pNLLuc (an Env-defective $HIV\text{-}1_{NL4\text{-}3}$ carrying the luciferase gene) (57) and either tetraspanin-expressing plasmids or empty vector. To prepare β-lactamase (BlaM)-conjugated Vpr-containing NL4-3 ($NL4\text{-}3^{BlaM\text{-}Vpr}$), pNL4-3 and pCMV4-3BlaM-Vpr (kindly provided by W. C. Greene) (8) were cotransfected with pCD63 or empty vector. To prepare $HIV\text{-}1_{IIIB}$, culture supernatants of Molt4/IIIB cells were harvested, centrifuged, and then filtered to produce virus solutions.

Antibodies and reagents. The following antibodies and reagents were used in this study: anti-CD63 mouse monoclonal antibody (mMAb) (MX-49.129.5; Santa Cruz Biotechnology, Santa Cruz, CA); anti-CD9 mMAb (M-L13; BD Biosciences, San Jose, CA); anti-CD81 mMAb (1D6; Serotec, Oxford, United Kingdom); anti-CD82 mMAb (B-L2; Serotec); anti-CD231 mMAb (H1-A12; BD Biosciences); anti-L6 mMAb (D1-D2; Chemicon, Temecula, CA); anti-CD45 mMAb (H130; BD Biosciences); anti-β-actin mMAb (AC-15; Sigma, St. Louis, MO); rat anti-gp120 MAb (W#10, which recognizes the V3 region of HIV_{IIIB} Env [Y. Tanaka, unpublished data]); goat anti-$p24^{CA}$ antiserum (ViroStat, Portland, ME); anti-$p17^{MA}$ mMAb (Applied Biotechnologies, Columbia, MD), which recognizes $p17^{MA}$ but not $Pr55^{Gag}$ (51); anti-Vpr mMAb (8D1; kindly donated by Y. Ishizaka); biotinylated horse anti-mouse immunoglobulin G (IgG) Ab (Vector Laboratories, Burlingame, CA); biotinylated donkey anti-rat IgG Ab (Rockland, Gilbertsville, PA); biotinylated donkey anti-goat IgG Ab (Chemicon); biotinylated donkey anti-rabbit IgG Ab (Chemicon); horseradish peroxidase-conjugated horse anti-mouse IgG Ab (Cell Signaling, Denver, MA); horseradish peroxidase-conjugated streptavidin (SA; Zymed, San Francisco, CA); and Alexa Fluor 488-conjugated goat anti-mouse IgG Ab (Molecular Probes, Eugene, OR).

Flow cytometry. In brief, cells were suspended in phosphate-buffered saline (PBS) and incubated for 30 min with appropriate antibodies at 4°C. Flow cytometry was performed with a FACScan (BD Biosciences), and data were analyzed using CellQuest software (BD Biosciences).

Immunoelectron microscopy. Cells were fixed with 0.2% glutaraldehyde in 150 mM PBS (pH 7.2) for 3 min at room temperature and harvested. The collected cells were fixed again with 1% glutaraldehyde in 150 mM PBS at 4°C for 60 min, dehydrated in a graded ethanol series, and embedded in Lowicryl K4M resin. Ultrathin sections were prepared using an ultramicrotome Reichert-Nissei Ul-

Downloaded from jvi.asm.org at Kyoto University on March 10, 2009

tracut-N (Leica, Vienna, Austria), and mounted on a nickel grid supported by a carbon-coated collodion film. The sections on the grid were treated with 5% goat serum in 150 mM PBS (pH 7.2) to block nonspecific reactions. The sections were treated with anti-CD63 mMAb at room temperature for 180 min. After washing three times, the sections were treated with goat serum containing 5-nm colloidal gold-labeled anti-mouse IgG (Amersham, Little Chalfont, United Kingdom) at room temperature for 60 min and washed in PBS. The immunostained sections were fixed with 1% glutaraldehyde in 50 mM cacodylate buffer again and washed in distilled water. The immunolabeled sections were treated with a mixture of 0.01% ruthenium red and 0.5% osmium tetroxide in 50 mM cacodylate buffer at room temperature for 10 min and double stained with uranyl acetate for 20 min, as previously described (38). The sections were observed under an electron microscope (H-7650; Hitachi, Ibaraki, Japan).

Western blotting and slot blotting. Cells were lysed with lysis buffer (1% Triton X-100, 50 mM Tris-HCl [pH 8.0], 150 mM NaCl, and protease inhibitor complete cocktail [Roche]). Virions were concentrated by ultracentrifugation at 100,000 × *g* for 1 h at 4°C, and pellets were lysed with lysis buffer. For Western blotting, lysates were separated by sodium dodecyl sulfate-polyacrylamide gel electrophoresis and transferred to Immobilon transfer membranes (Millipore, Bedford, MA). For detection, appropriate antibodies were used. Slot blotting was performed with a Hybri-slot Manifold (Invitrogen), according to the manufacturer's instructions.

Virus titration. IIIB was titrated by 50% tissue culture infective dose ($TCID_{50}$), and the infectious units (IU) of NL4-3, JR-FL, and NLFLV3 were measured by Magi assay, as follows.

(i) $TCID_{50}$. Virus solutions ($HIV\text{-}1_{IIIB}$) were serially diluted with RPMI 1640, and each solution was inoculated onto 6×10^4 MT-4 cells in quadruplicate. The $TCID_{50}$ was calculated as previously described (31).

(ii) Magi assay. MAGIC-5 cells (3×10^4) were seeded into a 24-well plate, 24 h before infection. Virus solutions ($HIV\text{-}1_{NL4\text{-}3}$, $HIV\text{-}1_{JR\text{-}FL}$, and $HIV\text{-}1_{NLFLV3}$) were diluted appropriately, 200 μl of the solutions was inoculated onto MAGIC-5 cells, and cells were incubated for 2 h at 37°C in a CO_2 incubator. After infection, 1 ml of conditioned medium was added for quenching, and the culture was further incubated for 48 h under the same conditions. Cells were fixed in fixing solution (1% formaldehyde, 0.2% glutaraldehyde in PBS) at 48 h postinfection and then treated with staining solution (400 μg/ml X-Gal [5-bromo-4-chloro-3-indolyl-β-D-galactopyranoside], 4 mM potassium ferrocyanide, 4 mM potassium ferricyanide, 2 mM $MgCl_2$ in PBS). Blue-stained cells in each well were counted in five fields, and the IU were calculated as previously described (29).

ELISA. To quantify $p24^{CA}$ in virus solutions, an HIV-1 p24 antigen enzyme-linked immunosorbent assay (ELISA) kit (ZetroMetrix, Buffalo, NY) was used according to the manufacturer's instructions.

Virus precipitation assay. Virus immunoprecipitation was performed as described previously (21), with some modifications. In brief, virus solution (100 ng of $p24^{CA}$) in PBS containing 3% bovine serum albumin (BSA) was incubated with 1 μg of each Ab overnight at 4°C. To harvest the virus-Ab complex, 25 μl of Dynabeads protein G (Dynal) in 3% BSA in PBS was added, and the mixture was held for 30 min at room temperature. The captured viruses were then precipitated with a magnet, washed with 3% BSA in PBS, and lysed with lysis buffer. $p24^{CA}$ was quantified by ELISA, as described above, and the amount of bound virions was calculated.

Pseudotyped virus infection and luciferase assay. To measure the infectivity of NL4-3 Env, IIIB Env, and NL4-3ΔCT Env-pseudotyped virus, MAGIC-5 cells (2×10^5) or MT-4 cells (1.5×10^5) were incubated for 48 h in an aliquot of each virus solution, containing 5 ng or 0.5 ng of $p24^{CA}$. A solution of JR-FL Env-pseudotyped virus, containing 20 ng of $p24^{CA}$, was incubated with MAGIC-5 cells (1×10^5) for 72 h. A solution of VSV envelope glycoprotein (VSV-G)-pseudotyped virus, containing 0.5 ng of $p24^{CA}$, was incubated with both MAGIC-5 cells (2×10^5) and MT-4 cells (1.5×10^5) for 48 h. Activated primary $CD4^+$ T cells (1×10^6) were inoculated with NL4-3 Env-pseudotyped virus, containing 10 ng of $p24^{CA}$, and incubated for 48 h. The Picagene luciferase assay kit (Toyo Ink, Tokyo, Japan) was used to perform luciferase assays, following the manufacturer's protocols. Activity was measured with a 1420 ARVOSX multilabel counter (Perkin Elmer, Wellesley, MA) and normalized to the protein content of each lysate, measured with a Coomassie (Bradford) protein assay kit (Pierce, Rockford, IL). All experiments were performed in triplicate.

Virus attachment assay. The virus attachment assay was performed as described previously (66) with some modifications. In brief, MT-4 cells (2×10^5) were incubated for 2 h at 4°C with an aliquot of HIV-1 containing 10 ng of $p24^{CA}$. After the incubation, cells were washed once with chilled Dulbecco's modified Eagle medium and five times with chilled PBS before being lysed with lysis buffer. The amounts of $p24^{CA}$ in these lysates were determined by ELISA, as described above, and the amount of attached virions was calculated.

HIV-1 fusion assay. The HIV-1 fusion assay, which is based on the incorporation of β-lactamase–Vpr chimeric proteins (BlaM-Vpr) into virions and subsequent BlaM cleavage of a fluorescent dye (CCF2) present in target cells, was performed as described previously (8). In brief, MT-4 cells (5×10^5) were incubated for 3 h at 37°C in a CO_2 incubator, with aliquots of $NL4\text{-}3^{BlaM\text{-}Vpr}$ containing 100 ng of $p24^{CA}$. Cells were washed once with an equilibrated buffer (RPMI 1640 containing 10% FCS and 20 mM HEPES-NaOH [pH 7.4]) and then incubated in 100 μl of substrate loading buffer (2 μM CCF2-AM in the equilibrated buffer, prepared according to the manufacturer's instructions [Invitrogen]) for 1 h at room temperature. After washing twice with the equilibrated buffer, cells were incubated in an equilibrated buffer containing 2.5 mM probenecid (Sigma) for 7 h at room temperature, to allow the BlaM reaction to develop. Finally, cells were washed once with PBS and fixed in 1% formalin neutral buffer solution. The change in emission fluorescence of the CCF2 dye, following its cleavage by BlaM-Vpr, was monitored by flow cytometry with FACSAria (BD Biosciences). Data were analyzed with FACSDiva software (BD Biosciences) and evaluated as previously described (8).

Real-time PCR. The amount of HIV-1 reverse transcripts (RT) was determined as previously described (64). In brief, to completely remove contaminating transfected pNL4-3 plasmid DNA, the virus solution was preincubated with DNase I (3,500 U/ml; Takara Bio, Shiga, Japan) containing 10 mM $MgCl_2$ for 30 min at room temperature. MT-4 cells (4×10^5) were incubated for 2 h at 37°C with aliquots of HIV-1 containing 2 ng of $p24^{CA}$. After infection, the cells were vigorously washed and cultured for 3 or 6 h. DNA was extracted by the urea-lysis method, and 500 ng of DNA was used as the template. Real-time PCR was performed by using a 7500 real-time system (Applied Biosystems), and data were analyzed with 7500 system SDS software (Applied Biosystems) and evaluated as previously described (64).

Statistical analysis. Student's *t* test was used to determine statistical significance. *P* values of <0.05, <0.01, and <0.001 were considered significant.

RESULTS

Activation of Molt4/IIIB cells intensifies HIV-1 infectivity and eliminates CD63 from both the released virions and the plasma membrane. The activation stimulus causes augmentation of HIV-1 production (30, 74). We stimulated Molt4/IIIB cells, which persistently produce infectious $HIV\text{-}1_{IIIB}$ virions (39), with PHA and PMA and detected a threefold increase in the amount of $p24^{CA}$ released into the culture supernatant, as measured by ELISA (Fig. 1A). Interestingly, we also found that PHA/PMA activation significantly enhanced the infectivity of released $HIV\text{-}1_{IIIB}$ virions (Fig. 1B). We first suspected that it might have been caused by the increase in the amount of mature HIV-1 Env, gp120, incorporated into HIV-1 particles. However, as shown in Fig. 1C, there was little change in the amount of gp120. Instead, the virus precipitation assay (21) revealed a large reduction in the virion-incorporated CD63 (Fig. 1D). As one of negative controls for this assay, we used an anti-CD45 antibody. It has already been proven that CD45 is expressed on the plasma membrane of leukocytes but is hardly incorporated into HIV-1 particles (49, 69). As previously reported, this antibody did not capture HIV-1 particles (Fig. 1D), suggesting that our assay specifically captured CD63 protein on the released HIV-1 particles. Correspondingly, we observed that CD63 expression on the surface of Molt4/IIIB cells was significantly down-modulated following PHA/PMA activation (Fig. 1E and F). As we suspected that the decrease of CD63 on virus particles might be related to the enhancement of virus infectivity, in subsequent experiments, we investigated the role of CD63 in the modulation of HIV-1 infectivity.

CD63 is incorporated into virions in an Env-independent manner and reduces infectivity. To directly examine the po-

Downloaded from jvi.asm.org at Kyoto University on March 10, 2009

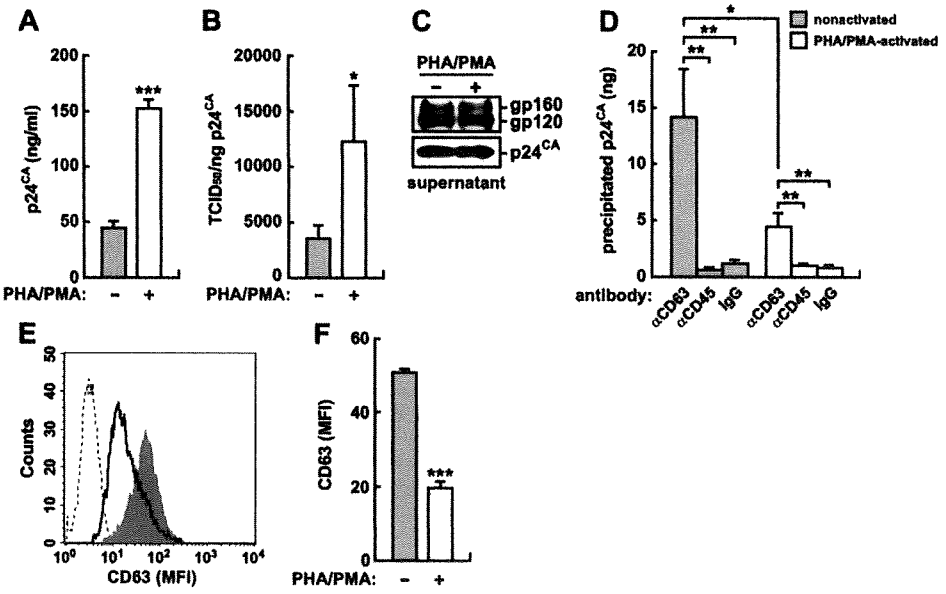

FIG. 1. Inverse correlation between HIV-1 infectivity and the level of CD63 in the released virions. Molt4/IIIB cells were activated with PHA (1 μg/ml) and PMA (100 ng/ml) for 72 h. (A) HIV-1_{IIIB} particles released from nonactivated or PHA/PMA-activated Molt4/IIIB cells were quantitated by $p24^{CA}$ ELISA. (B) The $TCID_{50}$ was measured as described in Materials and Methods and was normalized to the amount to $p24^{CA}$. (C) The level of Env in HIV-1_{IIIB} particles was analyzed by Western blotting. The input was standardized to $p24^{CA}$, and a representative result is shown. (D) The virus precipitation assay was performed as described in Materials and Methods. HIV-1_{IIIB} particles (100 ng of $p24^{CA}$) released from nonactivated or PHA/PMA-activated Molt4/IIIB cells were used for immunoprecipitation by respective antibodies. (E and F) The surface expression of CD63 on nonactivated (filled in gray) and PHA/PMA-activated (black line) Molt4/IIIB cells was analyzed by flow cytometry. Isotype IgG was used as a negative control (broken line). A representative result is shown in panel E, and summarized results are shown in panel F. Experiments were performed in triplicate. Statistical significance (Student's *t* test) is shown as follows: *, $P < 0.05$; **, $P < 0.01$; ***, $P < 0.001$. Error bars indicate standard deviations. MFI, mean fluorescence intensity.

tential of virion-incorporated CD63, we cotransfected a CD63 expression plasmid (pCD63) and pNL4-3 into 293T cells. Western blotting analyses showed that exogenous expression of CD63 did not influence the expression of HIV-1 components (Fig. 2A, top) and that there was little change in either the amount of released HIV-1 particles (Fig. 2C) or the detected HIV-1 components, including Env (gp120 and gp160), Gag (precursor protein [$Pr55^{Gag}$], cleavage intermediate [$p41^{MA\text{-}CA}$], $p24^{CA}$, and $p17^{MA}$), and Vpr (Fig. 2A, bottom). In addition, pNL4-3 transfection did not affect the surface expression of CD63, and exogenous CD63 was successfully expressed on the surfaces of 293T cells (Fig. 2B). In the virus precipitation assay, we observed that the level of endogenous CD63 on conventional HIV-$1_{NL4\text{-}3}$ particles (Fig. 2D) was similar to that on HIV-1_{IIIB} particles released from PHA/PMA-activated Molt4/IIIB cells (Fig. 1D). Likewise, exogenous CD63 was efficiently incorporated into the released HIV-$1_{NL4\text{-}3}$ (Fig. 2D) in amounts comparable to those in HIV-1_{IIIB} released from nonactivated Molt4/IIIB cells (Fig. 1D). These observations suggest that this 293T cell system may be an appropriate system for studying the phenomenon in Molt4/IIIB cells. Moreover, immunoelectron microscopy with an anti-CD63 antibody confirmed the presence of endogenous CD63 in HIV-1 particles (Fig. 2F), and the amount of virion-incorporated CD63 was increased by the exogenous expression (Fig. 2G). To analyze the necessity of Env for incorporation CD63 into released virions, we cotransfected cells with pCD63 and pNL4-3Δenv, which lacks NL4-3 *env* and produces virus-like particles. As shown in Fig. 2E, the level of CD63 on virus-like particles was comparable to that in wild-type NL4-3. Because ICAM-1 and HLA-DR are incorporated into released HIV-1 particles in an Env-independent manner (2, 44), it would not be surprising to find that Env is dispensable for the incorporation of CD63 into the released HIV-1 virions.

To investigate the virions released from pCD63-transfected cells further, we measured infectivity with a Magi assay (29). Although $p24^{CA}$ ELISA indicated that the amounts of released virions were comparable (Fig. 2C), the Magi assay revealed that the virions released from pCD63-transfected cells were significantly less infectious than typical virions (Fig. 2H). These results suggest that CD63 proteins on HIV-1 particles may have a suppressive effect on HIV-1 infection.

Non-virion-associated CD63 has no effect on HIV-1 infection. As shown in Fig. 2A, we observed that CD63 proteins are also released from the cells transfected solely with pCD63. It was recently reported that recombinant large extracellular domains of tetraspanin proteins, including CD63, potently inhibit HIV-1 infection (33). To eliminate the possibility that the infectivity reduction was caused by non-virion-associated CD63, we pretreated HIV-1 particles or target cells with the culture supernatant of the cells transfected solely with pCD63 (Fig. 3A) and evaluated the effect on HIV-1 infectivity by Magi assay. However, non-virion-associated CD63 did not affect HIV-1 infectivity (Fig. 3B to D). Moreover, we also examined whether non-virion-associated CD63 interferes with the virus precipitation assay. As shown in Fig. 3E, however, non-virion-associated CD63 did not affect virus precipitation by anti-

Downloaded from jvi.asm.org at Kyoto University on March 10, 2009

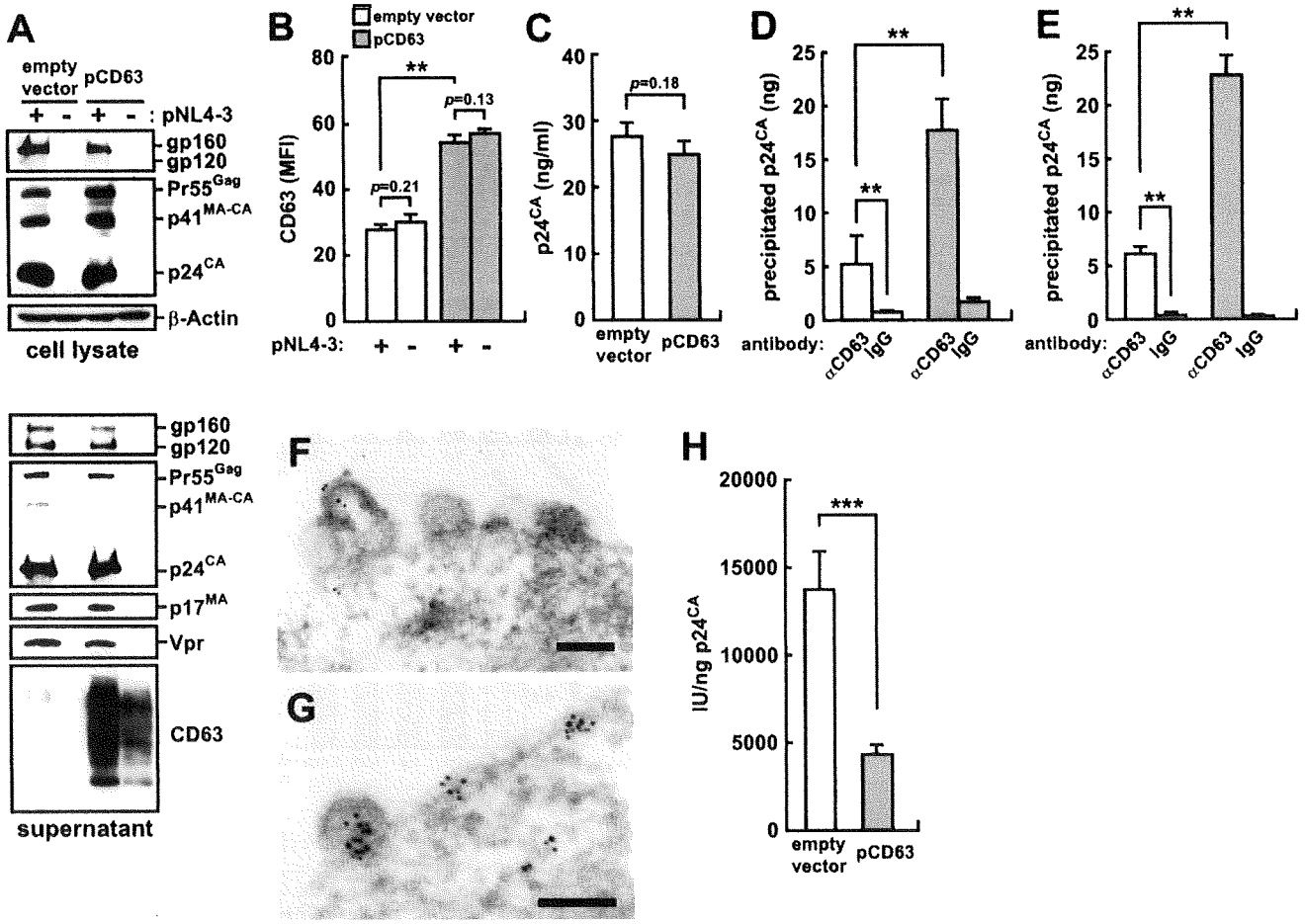

FIG. 2. Incorporation of exogenous CD63 into released HIV-1 virions and suppression of infectivity. Plasmid DNAs (pNL4-3 and either pCD63 or empty vector) were cotransfected into 293T cells as described in Materials and Methods. (A) Viral protein expression in the transfected 293T cells (cell lysate) and viral components in released HIV-1_{NL4-3} particles (supernatant) were analyzed by Western blotting, and a representative result is shown. The cell number was normalized to β-actin, and the released virions were harvested as described in Materials and Methods. (B) The surface expression of CD63 on empty vector-cotransfected and pCD63-cotransfected 293T cells was analyzed by flow cytometry. (C) The amount of released HIV-1_{NL4-3} particles released from empty vector-cotransfected or pCD63-cotransfected 293T cells was quantitated by $p24^{CA}$ ELISA. (D and E) HIV-1_{NL4-3} particles (D) and virus-like particles (E) (100 ng of $p24^{CA}$) released from empty vector-cotransfected or pCD63-cotransfected 293T cells were used for immunoprecipitation by respective antibodies, and the assay was performed as described in Materials and Methods. (F and G) Immunoelectron microscopy was performed as described in Materials and Methods. CD63 on HIV-1_{NL4-3} particles released from empty vector-cotransfected (F) and pCD63-cotransfected (G) 293T cells was detected by using anti-CD63 mouse antibody and was visualized with anti-mouse IgG 5-nm gold colloid (black dots). Bars, 100 nm. (H) IU of HIV-1_{NL4-3} released from empty vector-cotransfected or pCD63-cotransfected 293T cells were measured by Magi assay and were normalized to $p24^{CA}$. Experiments were performed in triplicate. Statistical significance (Student's *t* test) is shown as follows: **, $P < 0.01$; ***, $P < 0.001$. Error bars indicate standard deviations. MFI, mean fluorescence intensity.

CD63 antibody. In summary, the data suggest that only CD63 proteins incorporated into released virions have a role in the attenuation of HIV-1 infectivity.

CD63 on the cell surface is preferentially incorporated into the released virions. To investigate the correlation between HIV-1 infectivity and the level of CD63 on the released virions and on the surfaces of HIV-1-producing cells, we prepared pCD63ΔL, expressing a lysosomal target motif-deleted CD63. In agreement with a previous report (34), CD63ΔL was present in larger quantities on the cell surface than wild-type CD63 was (Fig. 4B), although the total amount of expressed protein was comparable to that of wild-type CD63 (Fig. 4A, top).

Using this plasmid, we investigated the effect of CD63ΔL on the infectivity of released virions. Although CD63ΔL did not affect the amount of either $p24^{CA}$ or gp120 released into the culture supernatant (Fig. 4A and C), it severely attenuated the infectivity of released NL4-3 (Fig. 4D). Furthermore, we noticed that CD63ΔL was incorporated into released virions in larger amounts than wild-type CD63 (Fig. 4E). These results suggest that infectivity is inversely correlated with the amount of CD63 (CD63ΔL) on both the released virions and the plasma membranes of HIV-1-producing cells.

Virion-incorporated CD63 impairs NL4-3 Env- and IIIB Env- but not JR-FL Env-mediated infection. To analyze the effect of virion-incorporated CD63 on other HIV-1 strains, we next cotransfected with pJR-FL and pCD63 into 293T cells. As in the case of NL4-3, exogenous CD63 did not affect the amount of released virions and was successfully incorporated

Downloaded from jvi.asm.org at Kyoto University on March 10, 2009

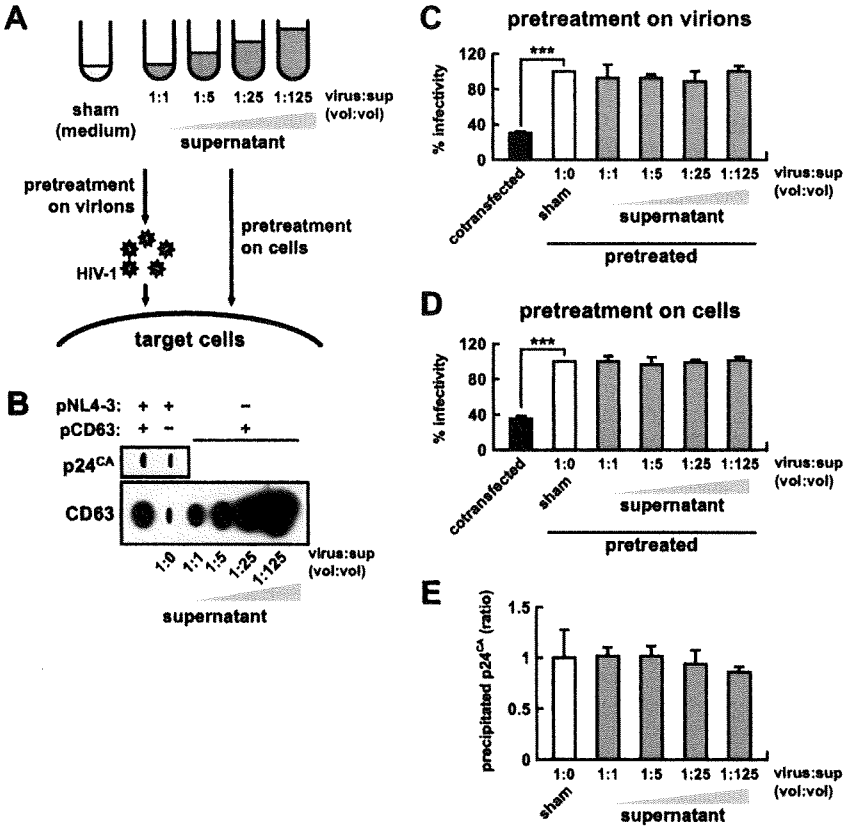

FIG. 3. Effect of non-virion-associated CD63. (A) Schematic diagram of the assay used for panels C and D. (B) Slot blotting shows the relative amounts of CD63 in each culture supernatant used for treatment. (C and D) Non-virion-associated CD63 was used to pretreat virions (C) or target cells (D), and the effect was assessed by Magi assay. RPMI 1640 was used as negative controls (sham), and the infectivity in controls was defined as 100%. The black bars indicate the infectivity of the virions released from the 293T cells cotransfected with pNL4-3 and pCD63, used as positive controls. (E) Effect of non-virion-associated CD63 in a virus precipitation assay. The amount of precipitated virions was quantified as described in Materials and Methods, and the ratio of amounts of precipitated virions to the sham-pretreated control was shown. The relative volumes of the supernatant shown schematically (A) and quantitatively (B) are identical to those used for panels C to E. Experiments were performed in triplicate. The *P* value versus sham-pretreated controls is <0.001 by Student's *t* test (***). Error bars indicate standard deviations.

into the released JR-FL (data not shown). However, virion-incorporated CD63 did not attenuate the infectivity of JR-FL (Fig. 5B).

NL4-3 uses CXCR4 as its coreceptor, whereas JR-FL uses CCR5, and coreceptor usage is severely dependent on the V3 region of Env (11). To investigate the possibility that the function of virion-incorporated CD63 is dependent on coreceptor usage, we used a chimeric HIV-1, NLFLV3. Although NLFLV3 uses CCR5 as its coreceptor (Fig. 5A) (18, 63), the infectivity of NLFLV3 was suppressed in a manner similar to that of wild-type NL4-3 (Fig. 5B). This result indicates that CD63 has the potential to reduce the infectivity of HIV-1 virions in a strain-specific manner and that it does not depend on coreceptor usage.

By cotransfecting pCD63 and pNLLuc, which has a defect in *env* and contains the luciferase gene (*luc*) in NL4-3 DNA, with Env (NL4-3 Env, IIIB Env, a CT-deleted NL4-3 [NL4-3ΔCT] Env, JR-FL Env, or VSV-G) expression plasmids, we prepared various pseudotyped viruses that each have Env on the *luc*-carrying particles. We observed that virion-incorporated CD63 suppressed the infectivity of viruses pseudotyped with NL4-3 Env (Fig. 6A) and IIIB Env (Fig. 6B) in a dose-dependent manner but did not affect that of viruses pseudotyped with JR-FL Env (Fig. 6D) and VSV-G (Fig. 6E). In addition, we found that the infectivity of viruses pseudotyped with NL4-3ΔCT Env was also attenuated through exogenous CD63 (Fig. 6C). Although it has been reported that the impediment of the association between Env CT and $p17^{MA}$ leads to repression of HIV-1 infection (16, 73), this result indicates that virion-incorporated CD63 does not affect the association of Env CT and $p17^{MA}$ at the lining of the viral membrane. Since the pseudotyped viruses differ only in Env, these results indicate that the effect of virion-incorporated CD63 is determined by Env. Moreover, the reduction in infectivity was also confirmed in activated primary $CD4^+$ T cells (Fig. 6F).

Virion-incorporated CD63 inhibits HIV-1 infection at the postattachment entry step(s). The process of HIV-1 entry into target cells has been extensively studied (23). The results described above indicate that virion-incorporated CD63 has the potential to disrupt NL4-3 and IIIB Env-mediated virus entry, and the disruption can negatively influence either attachment to CD4 on target cells or a conformational change of Env leading to virus-to-cell fusion mediated by gp41.

To address these possibilities, we initially compared the

Downloaded from jvi.asm.org at Kyoto University on March 10, 2009

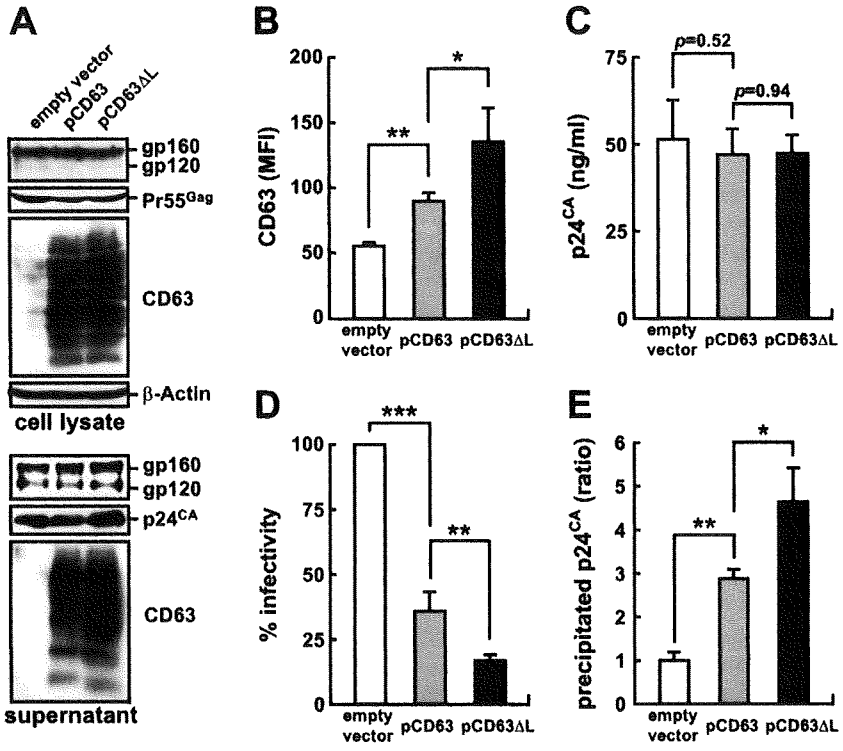

FIG. 4. Augmented reduction of the infectivity of released HIV-1 virions by CD63ΔL. Empty vector, pCD63, and pCD63ΔL were each cotransfected with pNL4-3 into 293T cells. (A) The expression of viral protein and CD63 in the transfected 293T cells and the components of released HIV-1_{NL4-3} particles were analyzed by Western blotting, and a representative result is shown. The cell number was normalized in comparison with β-actin, and the released virions were harvested as described in Materials and Methods. (B) The surface expression of CD63 on the transfected 293T cells was analyzed by flow cytometry. (C) The amount of released HIV-1_{NL4-3} particles was quantitated by $p24^{CA}$ ELISA. (D) IU of HIV-1_{NL4-3} was measured by Magi assay. The IU were normalized to the amount of $p24^{CA}$, and infectivity is shown as a percentage of the empty-vector value. (E) HIV-1_{NL4-3} particles (100 ng of $p24^{CA}$) were used for immunoprecipitation by anti-CD63 antibody. The ratio of precipitated virions to empty vector is shown. Experiments were performed in triplicate. Statistical significance (Student's *t* test) is shown as follows: *, $P < 0.05$; **, $P < 0.01$; ***, $P < 0.001$. Error bars indicate standard deviations. MFI, mean fluorescence intensity.

binding affinity of conventional and CD63-enriched virions. As shown in Fig. 7A, the binding affinity of CD63-enriched virions was not attenuated. To investigate the effect of CD63 on the HIV-1 fusion, we employed an enzyme-based HIV-1 fusion assay, involving preparation of BlaM-Vpr-containing virions (NL4-$3^{BlaM-Vpr}$), as described previously (8). Exogenous expression of CD63 had no effect on the amount of either virion-incorporated BlaM-Vpr or released virions, and CD63 was also successfully incorporated (data not shown). Using these virions, we studied the fusion of CD63-enriched virions by measuring the enzymatic activity of BlaM, which is taken up into the cytoplasm of target cells as a result of viral fusion. We observed that the uptake of BlaM, which reflects the fusion activity of viruses with target cells, was remarkably reduced in assays using CD63-enriched virions (Fig. 7B). The reduction in fusion efficiency

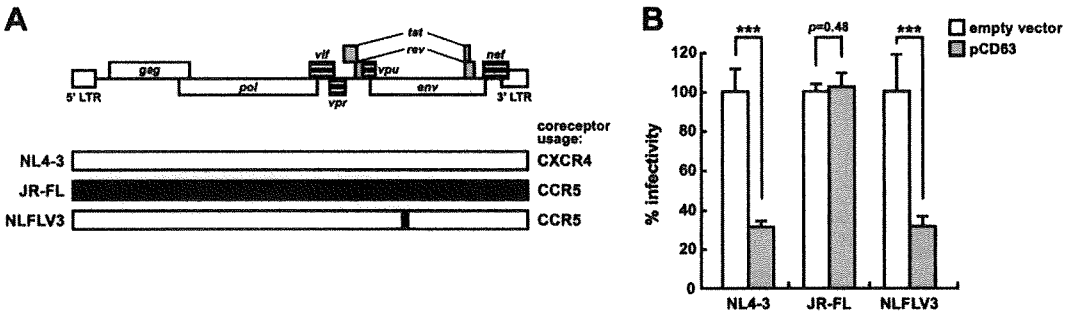

FIG. 5. Effect of virion-incorporated CD63 relative to other HIV-1 strains. (A) HIV-1 strains are schematically shown. (B) IU of respective viruses released from empty vector-cotransfected or pCD63-cotransfected 293T cells were measured by Magi assay. The IU were normalized to the amounts of $p24^{CA}$, and infectivity is shown as a percentage of the empty-vector value. Experiments were performed in triplicate. ***, $P < 0.001$ by Student's *t* test. Error bars indicate standard deviations.

Downloaded from jvi.asm.org at Kyoto University on March 10, 2009

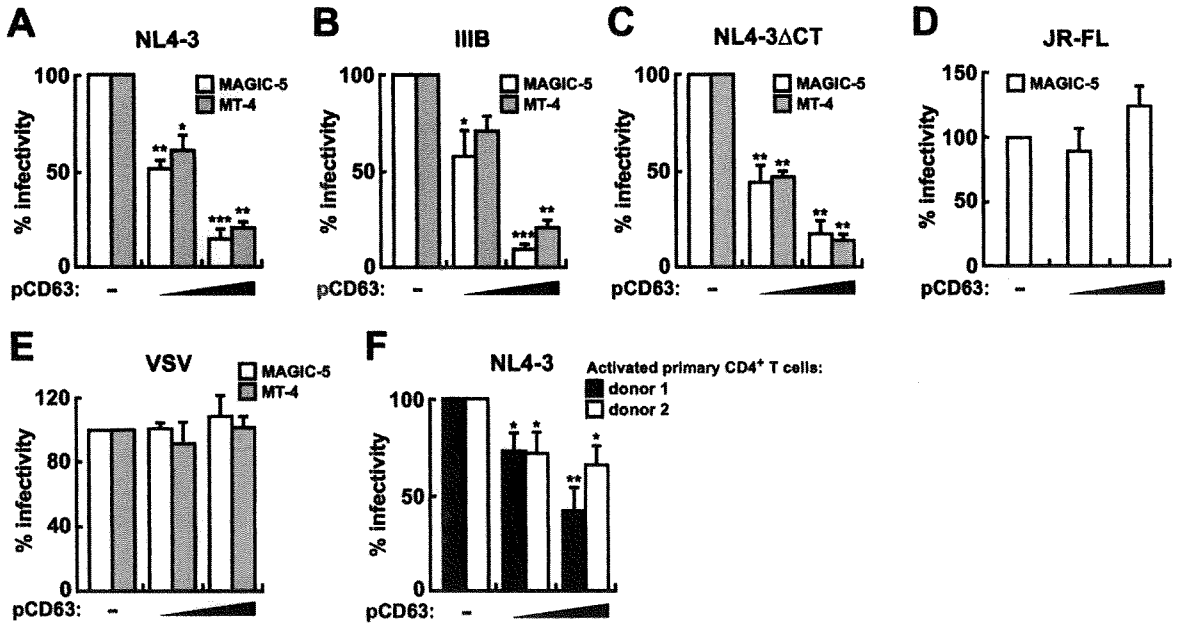

FIG. 6. Pseudotyped virus infection and luciferase assay. The prepared viruses were pseudotyped with Env of NL4-3 (A and F), IIIB (B), NL4-3ΔCT (C), JR-FL (D), or VSV (E). Each pseudotyped virus was prepared by cotransfection with pNLLuc, individual Env expression plasmids, and either empty vector or different doses of pCD63, as described in Materials and Methods. (A to E) MAGIC-5 cells and/or MT-4 cells were used as target cells. (F) NL4-3 Env-pseudotyped viruses were inoculated with CD3/CD28-activated primary $CD4^+$ T cells, and representative results are shown. The average luciferase activities per 1 μg of protein was calculated as relative light units, and infectivity is shown as a percentage of the empty-vector value. Experiments were performed in triplicate. Statistical significance (Student's *t* test) versus empty-vector values is shown as follows: *, $P < 0.05$; **, $P < 0.01$; ***; $P < 0.001$. Error bars indicate standard deviations.

corresponded closely to the reduction in infectivity (Fig. 2H). We also quantified HIV-1 RT by real-time PCR. As shown in Fig. 7C and D, both early and late RTs were decreased by CD63 enrichment. We concluded that virion-incorporated CD63 has the potential to prevent a postattachment step mediated by HIV-1 Env leading to the virus-to-cell fusion, and it causes the reduction in infectivity.

Tetraspanin proteins commonly have the potential to suppress HIV-1 infectivity. We analyzed the modulation of cell surface expression of other tetraspanins, CD9, CD81, CD82, and CD231, through cell activation. As shown in Fig. 8A, we observed that surface expression of other tetraspanins on Molt4/IIIB cells was also significantly down-modulated by PHA/PMA activation. Correlating with the surface expression, the amounts of virion-incorporated CD81, CD82, and CD231 were commonly decreased (Fig. 8B), although the amount of virion-incorporated CD9 was not significantly changed because of its lower level of incorporation.

Next, we cotransfected cells with pNL4-3 and individual tetraspanin (CD9, CD81, CD82, or CD231) expression plasmids. In addition, as a control protein, we also prepared an L6 expression plasmid. L6 has four transmembrane domains and is topologically similar to tetraspanins but does not belong to the genuine tetraspanin superfamily because of its structural

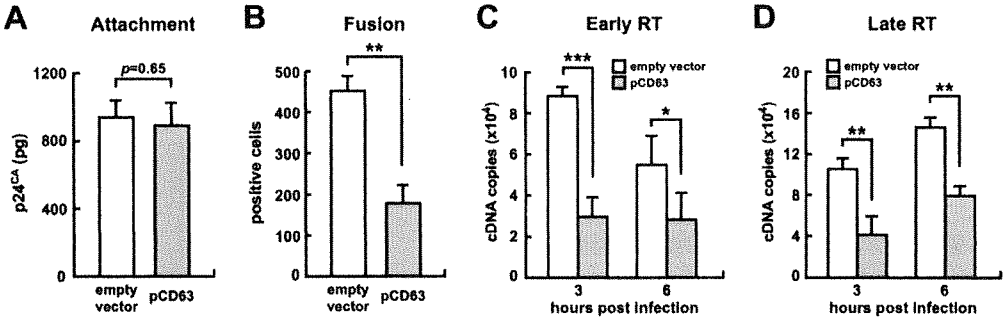

FIG. 7. Effect of virion-incorporated CD63 at early steps of HIV-1 infection. (A) Virus attachment assay. Aliquots of NL4-3 (10 ng of $p24^{CA}$) were incubated with MT-4 cells for 2 h at 4°C. After washing, the cells were lysed, and the amount of bound virions was quantitated by $p24^{CA}$ ELISA. A representative result is shown. (B) Virus fusion assay was performed as described in Materials and Methods, and the number of fused cells in 10,000 cells is shown. (C and D) Real-time PCR was performed as described in Materials and Methods, and the cDNA copy numbers of early (C) and late (D) RT in 100,000 cells are shown. Assays were performed in triplicate. Statistical significance (Student's *t* test) versus empty-vector values is shown as follows: *, $P < 0.05$; **, $P < 0.01$; ***, $P < 0.001$. Error bars indicate standard deviations.

Downloaded from jvi.asm.org at Kyoto University on March 10, 2009

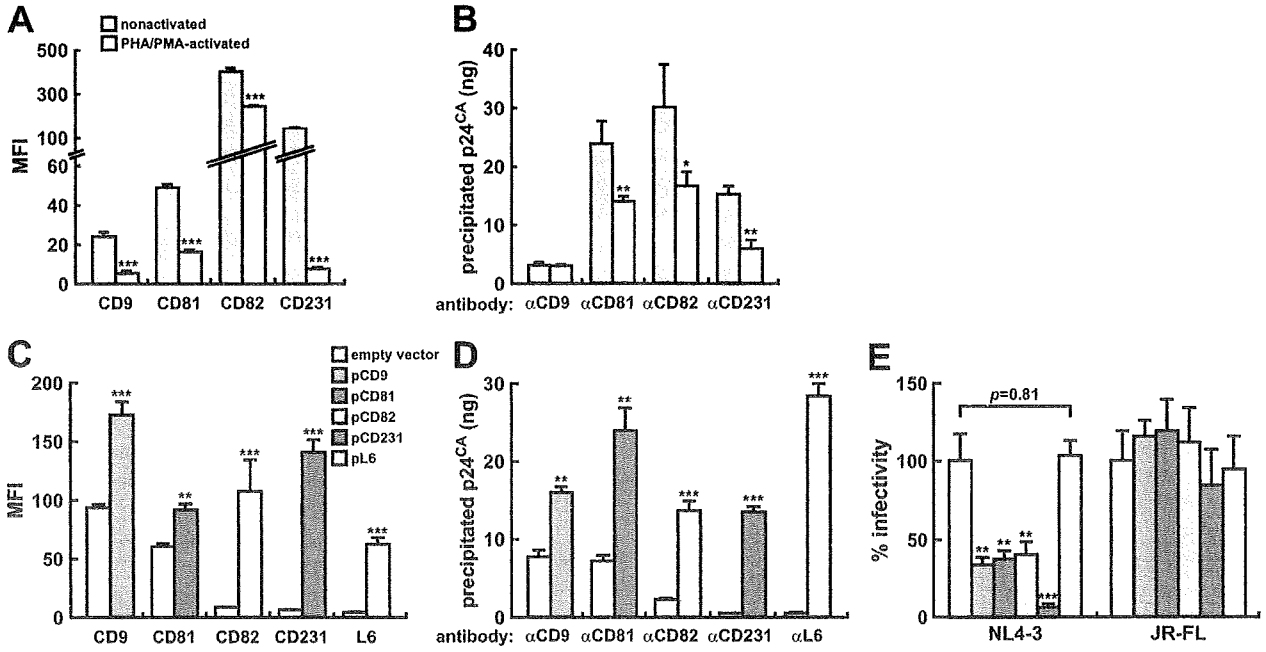

FIG. 8. Correlation between HIV-1 infectivity and the levels of tetraspanins in the released virions. (A and B) Molt4/IIIB cells were activated by PHA and PMA as described for Fig. 1. The surface expression of CD9, CD81, CD82, and CD231 on nonactivated and PHA/PMA-activated Molt4/IIIB cells was analyzed by flow cytometry. (B) The virus precipitation assay was performed as described in Materials and Methods. HIV-1_{IIIB} particles (100 ng of $p24^{CA}$) released from nonactivated or PHA/PMA-activated Molt4/IIIB cells were used for immunoprecipitation by respective antibodies. (C to E) Empty vector or individual tetraspanin-expression plasmids were each cotransfected with pNL4-3 into 293T cells. (C) The surface expression of tetraspanins on the 293T cells cotransfected with pNL4-3 and either empty vector or individual tetraspanin expression plasmids was analyzed by flow cytometry. (D) The virus precipitation assay was performed as described in Materials and Methods. HIV-1_{NL4-3} particles (100 ng of $p24^{CA}$) released from the 293T cells cotransfected with pNL4-3 and either empty vector or individual tetraspanin expression plasmids were used for immunoprecipitation by the respective antibodies. (E) IU of HIV-1_{NL4-3} or HIV-1_{JR-FL} released from the 293T cells cotransfected with pNL4-3 or pJR-FL and either empty vector or individual tetraspanin expression plasmids was measured by Magi assay. The IU were normalized to the amounts of $p24^{CA}$, and infectivity is shown as a percentage of empty-vector values. Experiments were performed in triplicate. Statistical significance compared to nonactivated (A and B) or empty vector (C to E) values (Student's *t* test) is shown as follows: *, $P < 0.05$; **, $P < 0.01$; ***, $P < 0.001$. Error bars indicate standard deviations. MFI, mean fluorescence intensity.

and evolutional divergence (68, 71). As shown in Fig. 8C, tetraspanins and L6 were expressed on the surface of 293T cells and did not modulate the surface expression of the other tetraspanin proteins (data not shown). Correlating with their surface expression, they were also efficiently incorporated into the released virions (Fig. 8D), as in the case of CD63 (Fig. 2). Furthermore, Magi assay revealed that CD9-, CD81-, CD82-, and CD231-enriched NL4-3 also had less infectivity (Fig. 8E). However, L6-enriched NL4-3 had infectivity comparable to that of typical NL4-3 (Fig. 8E). Interestingly, as found in the case of CD63, we also observed that virion-incorporated tetraspanins did not affect JR-FL infectivity (Fig. 8E). These results suggest that many tetraspanins have the potential to attenuate NL4-3 infectivity and that tetraspanins may cooperatively modulate its infectivity.

DISCUSSION

Various host membrane proteins, including CD63 and tetraspanin proteins, exist on HIV-1 particles (7, 9, 45, 46, 55), and some of them affect viral infection. For example, HLAs (6, 13, 44), costimulatory molecules (21, 25) and ICAM-1 (2, 4) enhance HIV-1 infectivity, while CD4 has the potential to suppress HIV-1 infection through incorporation into the released progeny virions (66). However, most of their functions for or against HIV-1 infection are still unclear. In this study, we quantitatively assessed CD63 incorporation into HIV-1 particles released from T cells and epithelial cell lines (Fig. 1 and 2) and examined its influence on the infectivity of the virions. In Molt4/IIIB cells, we found that a large quantity of CD63 was incorporated into the released particles (Fig. 1D). CD63 incorporation was reduced upon cellular activation (Fig. 1D), and this reduction was accompanied by increased infectivity (Fig. 1B). We showed that our CD63 exogenous expression model in 293T cells is useful for studying the relationship between CD63 incorporation and virion infectivity by demonstrating that pCD63-transfected 293T cells expressed amounts of surface CD63 (Fig. 2B) similar to those in nonactivated Molt4/IIIB cells (Fig. 1F) and that exogenous CD63 was also successfully incorporated into the released virions (Fig. 2D). Using this system, we showed that the infectivity of NL4-3 virions was not affected by released CD63 not associated with virus particles (Fig. 3). Rather, the infectivity of NL4-3 was inversely correlated with both the amount of virion-incorporated CD63 and the level of surface expression of CD63 (Fig. 4). In contrast to NL4-3 and IIIB, we found that JR-FL was resistant to CD63-mediated infectivity reduction (Fig. 5 and 6) and that Env determined the susceptibility to CD63 (Fig. 6). In

Downloaded from jvi.asm.org at Kyoto University on March 10, 2009

addition, virion-incorporated CD63 had the ability to impair HIV-1 entry without affecting the binding of Env to CD4 (Fig. 7). Furthermore, we found that other tetraspanin proteins, such as CD9, CD81, CD82, and CD231, all had the potential to be incorporated into released HIV-1 particles and to interfere with NL4-3 infection, as in the case of CD63, and that this potential is unique in tetraspanin proteins (Fig. 8). Taken together, these finding are the first indication that some host membrane proteins have the potential to modulate HIV-1 infectivity in a strain-specific manner through incorporation into released particles.

As shown in Fig. 1B, the infectivity of released HIV-1 virion was enhanced by Molt4/IIIB activation. Although the amounts of mature Env in released virions were comparable (Fig. 1C), we detected a decrease in the amount of virion-incorporated CD63 (Fig. 1D) and suspected that CD63 on virions has the potential to regulate HIV-1 infectivity. To confirm this possibility, we first attempted to decrease endogenous expression of CD63 through transfection with small interfering RNA against *cd63* in 293T cells. However, we could not detect significant differences in the infectivity of released HIV-1 virions (data not shown). We suspected that the lack of difference was due to the low level of endogenous CD63 in HIV-1 particles released from 293T cells (Fig. 2D), and we next planned to study its exogenous expression. Exogenous CD63 was successfully incorporated into the released particles (Fig. 2D). This level corresponded closely to the level of CD63 on IIIB virions released from nonactivated Molt4/IIIB cells (Fig. 1D; compare Fig. 2D) and also to the level described in a previous report (35). In addition, the amount of endogenous CD63 in NL4-3 particles released from 293T cells (Fig. 2D) also corresponded with that in IIIB particles released from PHA/PMA-activated Molt4/IIIB cells (Fig. 1D; compare Fig. 2D). Because the level of surface CD63 as well as incorporated CD63 was comparable between two systems (Fig. 1F and 2B), this 293T system was adequate to simulate the physiological phenomenon observed in Molt4/IIIB cells.

As shown in Fig. 2H, we detected attenuation of NL4-3 infectivity released from pCD63-transfected 293T cells. It has been reported that surface CD4 impairs Env incorporation and reduces the infectivity of the released virions (12, 42). Surface CD63 might also reduce the infectivity by affecting incorporation of Env. However, exogenous CD63 did not impair either Env maturation (Fig. 2A, top) or Env incorporation (Fig. 2A, bottom). On the other hand, Wyma et al. reported that immature HIV-1 particles are less active for fusion with target cell than mature particles (72). Exogenous CD63 might attenuate the maturation of HIV-1 particles. However, we found that Gag cleavage was successful (Fig. 2A, bottom). Recently, Ho et al. reported that a soluble recombinant LEL of CD63 has an ability to prevent HIV-1 infection (33), and we detected release of non-virion-associated CD63 into the culture supernatant of pCD63-transfected cells (Fig. 2A, bottom, rightmost lane). It was suspected that non-virion-associated CD63 released into the culture supernatant affected HIV-1 infection. However, non-virion-associated CD63 had no effect on HIV-1 infection (Fig. 3). Non-virion-associated CD63, which would be embedded on exosome/microvesicle-like components, may be inaccessible, as previously seen in the soluble recombinant LEL (33). As shown quantitatively (Fig. 2D) and visually (Fig. 2F), we detected the existence of CD63 on the released particles, and the amount was increased through exogenous expression (Fig. 2D and G). In addition, we observed that CD63ΔL preferentially localized at the cell surface (Fig. 4B) (34), while the whole amount was comparable to that of wild-type CD63 (Fig. 4A). Furthermore, CD63ΔL was additively incorporated (Fig. 4E) and then severely suppressed the infectivity of released virions (Fig. 4D). From these results, the amount of CD63 at the surfaces of HIV-1-producing cells clearly correlated with the level of CD63 in virions and inversely correlated with the infectivity of progeny NL4-3 virions. Accordingly, it appears that CD63 at the cell surface has a greater potential to be efficiently incorporated into released virions, which leads to the reduction in infectivity. This preference is reminiscent of positive correlation between the level of ICAM-1 surface expression on HIV-1-producing cells and the level of ICAM-1 in HIV-1 virions (54), although the effects elicited by respective embedded proteins were completely opposite.

It is known that the tetraspanin proteins have high homology in their structures and amino acid sequences (32, 62). Consistent with this observation, we found that exogenous tetraspanin proteins, such as CD9, CD81, CD82, and CD231, were also efficiently expressed at the cell surface (Fig. 8C) and can be incorporated into released NL4-3 particles and interfere with their infection (Fig. 8D and E). In contrast, a transmembrane protein called L6, which has four transmembrane domains but does not belong to the tetraspanin superfamily (68, 71), was also expressed at the cell surface and incorporated into the released particles (Fig. 8C and D) but did not affect HIV-1 infection (Fig. 8E). Actually, it has been reported that soluble LELs of other tetraspanin proteins, such as CD9, CD81, and CD82, also have the potential to suppress HIV-1 infection (33). Therefore, our findings clearly suggest that this is a common role for tetraspanins.

We observed that virion-incorporated CD63 did not affect JR-FL infectivity (Fig. 5B). In addition, through a pseudotyped-virus infection assay, we found that exogenous CD63 impaired the infection mediated by NL4-3 Env (Fig. 6A) and IIIB Env (Fig. 6B) in a dose-dependent manner and independently of the target cells (as shown in Fig. 6F, it was also confirmed in primary activated $CD4^+$ T cells). In contrast, there were no effects on the infection mediated by JR-FL Env (Fig. 6D) and VSV-G (Fig. 6E), although exogenous CD63 was incorporated into released particles in an Env-independent manner (Fig. 2E). These results indicate that susceptibility to CD63 is determined in Env and that there is strain specificity. There is a well-known difference between NL4-3 and JR-FL in their coreceptor usage: the former uses CXCR4 and the latter uses CCR5, and coreceptor preference is determined by the V3 region of Env (66). Since the infectivity reduction could be V3 region dependent, we further used NLFLV3 that contains the V3 region of JR-FL Env in NL4-3 Env and uses CCR5 as the coreceptor. However, the difference in the susceptibility for virion-incorporated CD63 between NL4-3 and JR-FL was not caused by the difference in coreceptor usage (Fig. 5B). Actually, other R5 viruses, such as JR-CSF and several chimeras, were also susceptible to CD63 (data not shown). In this regard, it is interesting that there is a difference in CD63 susceptibility between two R5 HIV-1 strains, JR-FL and JR-CSF, which were simultaneously isolated from the brain of an HIV-1 en-

Downloaded from jvi.asm.org at Kyoto University on March 10, 2009

cephalopathy patient (40). While the determinant region(s) in Env for the vulnerability to virion-incorporated CD63 has not been identified, these results indicate that there is some kind of strain specificity, or that JR-FL Env has some resistant property against virion-incorporated tetraspanins. It has been reported that a trivial change in Env conformation caused by mutation of one or more amino acid residues is responsible for the resistance to neutralizing antibodies and anti-HIV-1 drugs and that there are trivial differences in Env conformation between HIV-1 strains (5, 58). However, the crystal structure of the entire HIV-1 Env is not yet resolved, and it is difficult to speculate accurately on the invisible conformation of Env from its amino acid sequence. Our findings shed light on an unknown difference(s) between HIV-1 Envs, which is possibly conformational. Therefore, our findings may provide a clue for elucidating the ambiguous conformation of HIV-1 Env, which may lead to a novel target of anti-HIV drugs.

It has been reported that CD4 has the potential to inhibit HIV-1 infection at the attachment step through incorporation into the released HIV-1 particles (66). In contrast, as shown in Fig. 7A, virion-incorporated CD63 did not affect the attachment step. Rather, a postattachment step was attenuated by CD63 enrichment (Fig. 7B to D). It has been reported that the correct interaction between gp41 CT and $p17^{MA}$ in progeny virions is important to elicit efficient conformational changes of HIV-1 Env, leading to infection (14, 16, 72, 73). Virion-incorporated CD63 may disturb the interaction between gp41 CT and $p17^{MA}$ at the lining of virions. However, the infectivity of a CT-deleted NL4-3 Env-pseudotyped virus was also decreased by exogenous CD63 (Fig. 6C), suggesting that virion-incorporated CD63 had no or little effect on the interior of progeny virions. Interestingly, there are several reports showing that tetraspanin proteins are associated with physiological membrane fusion events. For example, murine CD9 on oocytes contributes to sperm-egg fusion (43, 47), and CD9 and CD81 on mononuclear phagocytes prevent their mutual fusion (65). In the case of human retroviruses, it was recently reported that the syncytium formation mediated by HIV-1 Env is suppressed by overexpression of CD9 and CD81 on the target cells (26). We think this is yet another phenomenon in which tetraspanin proteins are involved. Actually, tetraspanin proteins are able to interact laterally with each other through their LELs (62). Hence, CD63 on HIV-1 virion may laterally interact with endogenous CD9 and CD81 on target cells and may constitute an obstacle that impairs the stable interaction between gp120 and CD4/coreceptors following attachment.

Interestingly, PHA/PMA activation of Molt4/IIIB cells enhanced the infectivity of released IIIB virions (Fig. 1B), while the amount of incorporated Env was not changed (Fig. 1C). In this situation, it was interesting that the amount of virion-incorporated tetraspanins was decreased (Fig. 1D and 8B) and that their surface expression was significantly down-regulated (Fig. 1F and 8A). There was a clear relationship between the infectivity of released HIV-1 virions and the amount of tetraspanin proteins on both the virion and the surfaces of HIV-1-producing cells. Therefore, the enhancement of IIIB infectivity upon PHA/PMA activation of Molt4/IIIB cells should be at least partially due to the down-regulation of tetraspanin proteins.

Recently, the importance of tetraspanin proteins in HIV-1 replication has been recognized (3, 26, 50). The so-called "Trojan exosome hypothesis" proposes that HIV-1 applies TEMs and the machineries of exosome biosynthesis to its extracellular egress (27). However, the results we present here suggest that CD63 and other tetraspanins on viral membranes also have the potential to interfere with viral infection. The fundamental roles of tetraspanins and cellular membrane proteins in HIV-1 virions are intriguing, and further studies will be needed to uncover their mechanisms of action.

ACKNOWLEDGMENTS

We thank T. Murakami (AIDS Research Center, National Institute of Infectious Diseases), E. O. Freed (HIV Drug Resistance Program, National Cancer Institute-Frederick), Y. Ishizaka (Department of Intractable Diseases, International Medical Center of Japan), E. Mekada (Research Institute for Microbial Disease, Osaka University), W. A. O'Brien (Department of Microbiology and Immunology, University of Texas Medical Branch), and W. C. Greene (Gladstone Institute of Virology and Immunology, University of California) for providing materials required for this study. We are also grateful to the following colleagues from the Institute for Virus Research, Kyoto University, and Osaka Medical College: Yoshiharu Miura, Tomoko Kobayashi, and Yoshihiko Fujioka for instruction and support of experimental techniques, Youichi Suzuki for helpful suggestions, Chuanyi Nie for proofreading of the manuscript, and Takeshi Yoshida for lively discussions.

This work was supported by grants from the Ministry of Health, Labor and Welfare and the Ministry of Education, Culture, Sports, Science and Technology of Japan.

REFERENCES

1. **Adachi, A., H. E. Gendelman, S. Koenig, T. Folks, R. Willey, A. Rabson, and M. A. Martin.** 1986. Production of acquired immunodeficiency syndrome-associated retrovirus in human and nonhuman cells transfected with an infectious molecular clone. J. Virol. **59:**284–291.
2. **Beausejour, Y., and M. J. Tremblay.** 2004. Envelope glycoproteins are not required for insertion of host ICAM-1 into human immunodeficiency virus type 1 and ICAM-1-bearing viruses are still infectious despite a suboptimal level of trimeric envelope proteins. Virology **324:**165–172.
3. **Booth, A. M., Y. Fang, J. K. Fallon, J. M. Yang, J. E. Hildreth, and S. J. Gould.** 2006. Exosomes and HIV Gag bud from endosome-like domains of the T cell plasma membrane. J. Cell Biol. **172:**923–935.
4. **Bounou, S., J. E. Leclerc, and M. J. Tremblay.** 2002. Presence of host ICAM-1 in laboratory and clinical strains of human immunodeficiency virus type 1 increases virus infectivity and $CD4^+$-T-cell depletion in human lymphoid tissue, a major site of replication in vivo. J. Virol. **76:**1004–1014.
5. **Burton, D. R.** 1997. A vaccine for HIV type 1: the antibody perspective. Proc. Natl. Acad. Sci. USA **94:**10018–10023.
6. **Cantin, R., J. F. Fortin, G. Lamontagne, and M. Tremblay.** 1997. The presence of host-derived HLA-DR1 on human immunodeficiency virus type 1 increases viral infectivity. J. Virol. **71:**1922–1930.
7. **Cantin, R., S. Methot, and M. J. Tremblay.** 2005. Plunder and stowaways: incorporation of cellular proteins by enveloped viruses. J. Virol. **79:**6577–6587.
8. **Cavrois, M., C. De Noronha, and W. C. Greene.** 2002. A sensitive and specific enzyme-based assay detecting HIV-1 virion fusion in primary T lymphocytes. Nat. Biotechnol. **20:**1151–1154.
9. **Chertova, E., O. Chertov, L. V. Coren, J. D. Roser, C. M. Trubey, J. W. Bess, Jr., R. C. Sowder, I. I., E. Barsov, B. L. Hood, R. J. Fisher, K. Nagashima, T. P. Conrads, T. D. Veenstra, J. D. Lifson, and D. E. Ott.** 2006. Proteomic and biochemical analysis of purified human immunodeficiency virus type 1 produced from infected monocyte-derived macrophages. J. Virol. **80:**9039–9052.
10. **Choe, H., M. Farzan, Y. Sun, N. Sullivan, B. Rollins, P. D. Ponath, L. Wu, C. R. Mackay, G. LaRosa, W. Newman, N. Gerard, C. Gerard, and J. Sodroski.** 1996. The β-chemokine receptors CCR3 and CCR5 facilitate infection by primary HIV-1 isolates. Cell **85:**1135–1148.
11. **Cocchi, F., A. L. DeVico, A. Garzino-Demo, A. Cara, R. C. Gallo, and P. Lusso.** 1996. The V3 domain of the HIV-1 gp120 envelope glycoprotein is critical for chemokine-mediated blockade of infection. Nat. Med. **2:**1244–1247.
12. **Cortes, M. J., F. Wong-Staal, and J. Lama.** 2002. Cell surface CD4 interferes with the infectivity of HIV-1 particles released from T cells. J. Biol. Chem. **277:**1770–1779.
13. **Cosma, A., D. Blanc, J. Braun, C. Quillent, C. Barassi, C. Moog, S. Klasen,**

Downloaded from jvi.asm.org at Kyoto University on March 10, 2009

B. Spire, G. Scarlatti, E. Pesenti, A. G. Siccardi, and A. Beretta. 1999. Enhanced HIV infectivity and changes in GP120 conformation associated with viral incorporation of human leucocyte antigen class I molecules. AIDS **13:**2033–2042.

14. **Cosson, P.** 1996. Direct interaction between the envelope and matrix proteins of HIV-1. EMBO J. **15:**5783–5788.
15. **Dalgleish, A. G., P. C. Beverley, P. R. Clapham, D. H. Crawford, M. F. Greaves, and R. A. Weiss.** 1984. The CD4 (T4) antigen is an essential component of the receptor for the AIDS retrovirus. Nature **312:**763–767.
16. **Davis, M. R., J. Jiang, J. Zhou, E. O. Freed, and C. Aiken.** 2006. A mutation in the human immunodeficiency virus type 1 Gag protein destabilizes the interaction of the envelope protein subunits gp120 and gp41. J. Virol. **80:** 2405–2417.
17. **Deng, H., R. Liu, W. Ellmeier, S. Choe, D. Unutmaz, M. Burkhart, P. Di Marzio, S. Marmon, R. E. Sutton, C. M. Hill, C. B. Davis, S. C. Peiper, T. J. Schall, D. R. Littman, and N. R. Landau.** 1996. Identification of a major co-receptor for primary isolates of HIV-1. Nature **381:**661–666.
18. **Derdeyn, C. A., J. M. Decker, J. N. Sfakianos, X. Wu, W. A. O'Brien, L. Ratner, J. C. Kappes, G. M. Shaw, and E. Hunter.** 2000. Sensitivity of human immunodeficiency virus type 1 to the fusion inhibitor T-20 is modulated by coreceptor specificity defined by the V3 loop of gp120. J. Virol. **74:**8358–8367.
19. **Doranz, B. J., J. Rucker, Y. Yi, R. J. Smyth, M. Samson, S. C. Peiper, M. Parmentier, R. G. Collman, and R. W. Doms.** 1996. A dual-tropic primary HIV-1 isolate that uses fusin and the β-chemokine receptors CKR-5, CKR-3, and CKR-2b as fusion cofactors. Cell **85:**1149–1158.
20. **Dragic, T., V. Litwin, G. P. Allaway, S. R. Martin, Y. Huang, K. A. Nagashima, C. Cayanan, P. J. Maddon, R. A. Koup, J. P. Moore, and W. A. Paxton.** 1996. HIV-1 entry into $CD4^+$ cells is mediated by the chemokine receptor CC-CKR-5. Nature **381:**667–673.
21. **Esser, M. T., D. R. Graham, L. V. Coren, C. M. Trubey, J. W. Bess, Jr., L. O. Arthur, D. E. Ott, and J. D. Lifson.** 2001. Differential incorporation of CD45, CD80 (B7-1), CD86 (B7-2), and major histocompatibility complex class I and II molecules into human immunodeficiency virus type 1 virions and microvesicles: implications for viral pathogenesis and immune regulation. J. Virol. **75:**6173–6182.
22. **Feng, Y., C. C. Broder, P. E. Kennedy, and E. A. Berger.** 1996. HIV-1 entry cofactor: functional cDNA cloning of a seven-transmembrane, G protein-coupled receptor. Science **272:**872–877.
23. **Freed, E. O., and M. A. Martin.** 2001. HIVs and their replication, p. 1971–2041. *In* D. M. Knipe and P. M. Howley (ed.), Fields virology, 4th ed., vol. 2. Lippincott Williams & Wilkins, Philadelphia, PA.
24. **Freed, E. O., and M. A. Martin.** 1995. The role of human immunodeficiency virus type 1 envelope glycoproteins in virus infection. J. Biol. Chem. **270:** 23883–23886.
25. **Giguere, J. F., S. Bounou, J. S. Paquette, J. Madrenas, and M. J. Tremblay.** 2004. Insertion of host-derived costimulatory molecules CD80 (B7.1) and CD86 (B7.2) into human immunodeficiency virus type 1 affects the virus life cycle. J. Virol. **78:**6222–6232.
26. **Gordon-Alonso, M., M. Yanez-Mo, O. Barreiro, S. Alvarez, M. A. Munoz-Fernandez, A. Valenzuela-Fernandez, and F. Sanchez-Madrid.** 2006. Tetraspanins CD9 and CD81 modulate HIV-1-induced membrane fusion. J. Immunol. **177:**5129–5137.
27. **Gould, S. J., A. M. Booth, and J. E. Hildreth.** 2003. The Trojan exosome hypothesis. Proc. Natl. Acad. Sci. USA **100:**10592–10597.
28. **Grigorov, B., F. Arcanger, P. Roingeard, J. L. Darlix, and D. Muriaux.** 2006. Assembly of infectious HIV-1 in human epithelial and T-lymphoblastic cell lines. J. Mol. Biol. **359:**848–862.
29. **Hachiya, A., S. Aizawa-Matsuoka, M. Tanaka, Y. Takahashi, S. Ida, H. Gatanaga, Y. Hirabayashi, A. Kojima, M. Tatsumi, and S. Oka.** 2001. Rapid and simple phenotypic assay for drug susceptibility of human immunodeficiency virus type 1 using CCR5-expressing HeLa/$CD4^+$ cell clone 1–10 (MAGIC-5). Antimicrob. Agents Chemother. **45:**495–501.
30. **Harada, S., Y. Koyanagi, H. Nakashima, N. Kobayashi, and N. Yamamoto.** 1986. Tumor promoter, TPA, enhances replication of HTLV-III/LAV. Virology **154:**249–258.
31. **Harada, S., Y. Koyanagi, and N. Yamamoto.** 1985. Infection of HTLV-III/LAV in HTLV-I-carrying cells MT-2 and MT-4 and application in a plaque assay. Science **229:**563–566.
32. **Hemler, M. E.** 2005. Tetraspanin functions and associated microdomains. Nat. Rev. Mol. Cell Biol. **6:**801–811.
33. **Ho, S. H., F. Martin, A. Higginbottom, L. J. Partridge, V. Parthasarathy, G. W. Moseley, P. Lopez, C. Cheng-Mayer, and P. N. Monk.** 2006. Recombinant extracellular domains of tetraspanin proteins are potent inhibitors of the infection of macrophages by human immunodeficiency virus type 1. J. Virol. **80:**6487–6496.
34. **Janvier, K., and J. S. Bonifacino.** 2005. Role of the endocytic machinery in the sorting of lysosome-associated membrane proteins. Mol. Biol. Cell **16:** 4231–4242.
35. **Jolly, C., and Q. J. Sattentau.** 2007. Human immunodeficiency virus type 1 assembly, budding, and cell-cell spread in T cells take place in tetraspanin-enriched plasma membrane domains. J. Virol. **81:**7873–7884.
36. **Kawano, Y., T. Yoshida, K. Hieda, J. Aoki, H. Miyoshi, and Y. Koyanagi.** 2004. A lentiviral cDNA library employing lambda recombination used to clone an inhibitor of human immunodeficiency virus type 1-induced cell death. J. Virol. **78:**11352–11359.
37. **Klatzmann, D., E. Champagne, S. Chamaret, J. Gruest, D. Guetard, T. Hercend, J. C. Gluckman, and L. Montagnier.** 1984. T-lymphocyte T4 molecule behaves as the receptor for human retrovirus LAV. Nature **312:**767–768.
38. **Kohno, T., Y. Fujioka, T. Goto, S. Morimatsu, C. Morita, T. Nakano, and K. Sano.** 1998. Contrast-enhancement for the image of human immunodeficiency virus from ultrathin section by immunoelectron microscopy. J. Virol. Methods **72:**137–143.
39. **Koyanagi, Y., S. Harada, and N. Yamamoto.** 1986. Establishment of a high production system for AIDS retroviruses with a human T-leukemic cell line Molt-4. Cancer Lett. **30:**299–310.
40. **Koyanagi, Y., S. Miles, R. T. Mitsuyasu, J. E. Merrill, H. V. Vinters, and I. S. Chen.** 1987. Dual infection of the central nervous system by AIDS viruses with distinct cellular tropisms. Science **236:**819–822.
41. **Koyanagi, Y., Y. Tanaka, J. Kira, M. Ito, K. Hioki, N. Misawa, Y. Kawano, K. Yamasaki, R. Tanaka, Y. Suzuki, Y. Ueyama, E. Terada, T. Tanaka, M. Miyasaka, T. Kobayashi, Y. Kumazawa, and N. Yamamoto.** 1997. Primary human immunodeficiency virus type 1 viremia and central nervous system invasion in a novel hu-PBL-immunodeficient mouse strain. J. Virol. **71:**2417–2424.
42. **Lama, J., A. Mangasarian, and D. Trono.** 1999. Cell-surface expression of CD4 reduces HIV-1 infectivity by blocking Env incorporation in a Nef- and Vpu-inhibitable manner. Curr. Biol. **9:**622–631.
43. **Le Naour, F., E. Rubinstein, C. Jasmin, M. Prenant, and C. Boucheix.** 2000. Severely reduced female fertility in CD9-deficient mice. Science **287:**319–321.
44. **Martin, G., Y. Beausejour, J. Thibodeau, and M. J. Tremblay.** 2005. Envelope glycoproteins are dispensable for insertion of host HLA-DR molecules within nascent human immunodeficiency virus type 1 particles. Virology **335:**286–290.
45. **Meerloo, T., H. K. Parmentier, A. D. Osterhaus, J. Goudsmit, and H. J. Schuurman.** 1992. Modulation of cell surface molecules during HIV-1 infection of H9 cells. An immunoelectron microscopic study. AIDS **6:**1105–1116.
46. **Meerloo, T., M. A. Sheikh, A. C. Bloem, A. de Ronde, M. Schutten, C. A. van Els, P. J. Roholl, P. Joling, J. Goudsmit, and H. J. Schuurman.** 1993. Host cell membrane proteins on human immunodeficiency virus type 1 after in vitro infection of H9 cells and blood mononuclear cells. An immuno-electron microscopic study. J. Gen. Virol. **74:**129–135.
47. **Miyado, K., G. Yamada, S. Yamada, H. Hasuwa, Y. Nakamura, F. Ryu, K. Suzuki, K. Kosai, K. Inoue, A. Ogura, M. Okabe, and E. Mekada.** 2000. Requirement of CD9 on the egg plasma membrane for fertilization. Science **287:**321–324.
48. **Murakami, T., and E. O. Freed.** 2000. The long cytoplasmic tail of gp41 is required in a cell type-dependent manner for HIV-1 envelope glycoprotein incorporation into virions. Proc. Natl. Acad. Sci. USA **97:**343–348.
49. **Nguyen, D. H., and J. E. Hildreth.** 2000. Evidence for budding of human immunodeficiency virus type 1 selectively from glycolipid-enriched membrane lipid rafts. J. Virol. **74:**3264–3272.
50. **Nydegger, S., S. Khurana, D. N. Krementsov, M. Foti, and M. Thali.** 2006. Mapping of tetraspanin-enriched microdomains that can function as gateways for HIV-1. J. Cell Biol. **173:**795–807.
51. **Ono, A., S. D. Ablan, S. J. Lockett, K. Nagashima, and E. O. Freed.** 2004. Phosphatidylinositol (4,5) bisphosphate regulates HIV-1 Gag targeting to the plasma membrane. Proc. Natl. Acad. Sci. USA **101:**14889–14894.
52. **Ono, A., and E. O. Freed.** 2004. Cell-type-dependent targeting of human immunodeficiency virus type 1 assembly to the plasma membrane and the multivesicular body. J. Virol. **78:**1552–1563.
53. **Ory, D. S., B. A. Neugeboren, and R. C. Mulligan.** 1996. A stable human-derived packaging cell line for production of high titer retrovirus/vesicular stomatitis virus G pseudotypes. Proc. Natl. Acad. Sci. USA **93:**11400–11406.
54. **Paquette, J. S., J. F. Fortin, L. Blanchard, and M. J. Tremblay.** 1998. Level of ICAM-1 surface expression on virus producer cells influences both the amount of virion-bound host ICAM-1 and human immunodeficiency virus type 1 infectivity. J. Virol. **72:**9329–9336.
55. **Pelchen-Matthews, A., B. Kramer, and M. Marsh.** 2003. Infectious HIV-1 assembles in late endosomes in primary macrophages. J. Cell Biol. **162:**443–455.
56. **Perlman, M., and M. D. Resh.** 2006. Identification of an intracellular trafficking and assembly pathway for HIV-1 Gag. Traffic **7:**731–745.
57. **Planelles, V., F. Bachelerie, J. B. Jowett, A. Haislip, Y. Xie, P. Banooni, T. Masuda, and I. S. Chen.** 1995. Fate of the human immunodeficiency virus type 1 provirus in infected cells: a role for vpr. J. Virol. **69:**5883–5889.
58. **Poignard, P., E. O. Saphire, P. W. Parren, and D. R. Burton.** 2001. gp120: biologic aspects of structural features. Annu. Rev. Immunol. **19:**253–274.
59. **Poon, B., K. Grovit-Ferbas, S. A. Stewart, and I. S. Chen.** 1998. Cell cycle arrest by Vpr in HIV-1 virions and insensitivity to antiretroviral agents. Science **281:**266–269.
60. **Raposo, G., M. Moore, D. Innes, R. Leijendekker, A. Leigh-Brown, P. Bena-**

Downloaded from jvi.asm.org at Kyoto University on March 10, 2009

roch, and H. Geuze. 2002. Human macrophages accumulate HIV-1 particles in MHC II compartments. Traffic **3**:718–729.
61. **Saifuddin, M., C. J. Parker, M. E. Peeples, M. K. Gorny, S. Zolla-Pazner, M. Ghassemi, I. A. Rooney, J. P. Atkinson, and G. T. Spear.** 1995. Role of virion-associated glycosylphosphatidylinositol-linked proteins CD55 and CD59 in complement resistance of cell line-derived and primary isolates of HIV-1. J. Exp. Med. **182**:501–509.
62. **Stipp, C. S., T. V. Kolesnikova, and M. E. Hemler.** 2003. Functional domains in tetraspanin proteins. Trends Biochem. Sci. **28**:106–112.
63. **Suzuki, Y., Y. Koyanagi, Y. Tanaka, T. Murakami, N. Misawa, N. Maeda, T. Kimura, H. Shida, J. A. Hoxie, W. A. O'Brien, and N. Yamamoto.** 1999. Determinant in human immunodeficiency virus type 1 for efficient replication under cytokine-induced $CD4^+$ T-helper 1 (Th1)- and Th2-type conditions. J. Virol. **73**:316–324.
64. **Suzuki, Y., N. Misawa, C. Sato, H. Ebina, T. Masuda, N. Yamamoto, and Y. Koyanagi.** 2003. Quantitative analysis of human immunodeficiency virus type 1 DNA dynamics by real-time PCR: integration efficiency in stimulated and unstimulated peripheral blood mononuclear cells. Virus Genes **27**:177–188.
65. **Takeda, Y., I. Tachibana, K. Miyado, M. Kobayashi, T. Miyazaki, T. Funakoshi, H. Kimura, H. Yamane, Y. Saito, H. Goto, T. Yoneda, M. Yoshida, T. Kumagai, T. Osaki, S. Hayashi, I. Kawase, and E. Mekada.** 2003. Tetraspanins CD9 and CD81 function to prevent the fusion of mononuclear phagocytes. J. Cell Biol. **161**:945–956.
66. **Tanaka, M., T. Ueno, T. Nakahara, K. Sasaki, A. Ishimoto, and H. Sakai.** 2003. Downregulation of CD4 is required for maintenance of viral infectivity of HIV-1. Virology **311**:316–325.
67. **Tardif, M. R., and M. J. Tremblay.** 2003. Presence of host ICAM-1 in human immunodeficiency virus type 1 virions increases productive infection of $CD4^+$ T lymphocytes by favoring cytosolic delivery of viral material. J. Virol. **77**:12299–12309.
68. **Tarrant, J. M., L. Robb, A. B. van Spriel, and M. D. Wright.** 2003. Tetraspanins: molecular organisers of the leukocyte surface. Trends Immunol. **24**:610–617.
69. **Trubey, C. M., E. Chertova, L. V. Coren, J. M. Hilburn, C. V. Hixson, K. Nagashima, J. D. Lifson, and D. E. Ott.** 2003. Quantitation of HLA class II protein incorporated into human immunodeficiency type 1 virions purified by anti-CD45 immunoaffinity depletion of microvesicles. J. Virol. **77**:12699–12709.
70. **von Lindern, J. J., D. Rojo, K. Grovit-Ferbas, C. Yeramian, C. Deng, G. Herbein, M. R. Ferguson, T. C. Pappas, J. M. Decker, A. Singh, R. G. Collman, and W. A. O'Brien.** 2003. Potential role for CD63 in CCR5-mediated human immunodeficiency virus type 1 infection of macrophages. J. Virol. **77**:3624–3633.
71. **Wright, M. D., J. Ni, and G. B. Rudy.** 2000. The L6 membrane proteins—a new four-transmembrane superfamily. Protein Sci. **9**:1594–1600.
72. **Wyma, D. J., J. Jiang, J. Shi, J. Zhou, J. E. Lineberger, M. D. Miller, and C. Aiken.** 2004. Coupling of human immunodeficiency virus type 1 fusion to virion maturation: a novel role of the gp41 cytoplasmic tail. J. Virol. **78**: 3429–3435.
73. **Wyma, D. J., A. Kotov, and C. Aiken.** 2000. Evidence for a stable interaction of gp41 with $Pr55^{Gag}$ in immature human immunodeficiency virus type 1 particles. J. Virol. **74**:9381–9387.
74. **Zagury, D., J. Bernard, R. Leonard, R. Cheynier, M. Feldman, P. S. Sarin, and R. C. Gallo.** 1986. Long-term cultures of HTLV-III-infected T cells: a model of cytopathology of T-cell depletion in AIDS. Science **231**:850–853.

Downloaded from jvi.asm.org at Kyoto University on March 10, 2009

Traffic 2008; 9: 540–558
Blackwell Munksgaard

© 2008 The Authors
Journal compilation © 2008 Blackwell Publishing Ltd

doi: 10.1111/j.1600-0854.2007.00700.x

A CD63 Mutant Inhibits T-cell Tropic Human Immunodeficiency Virus Type 1 Entry by Disrupting CXCR4 Trafficking to the Plasma Membrane

Takeshi Yoshida[1], Yuji Kawano[2], Kei Sato[1], Yoshinori Ando[1], Jun Aoki[1], Yoshiharu Miura[1], Jun Komano[3], Yuetsu Tanaka[4] and Yoshio Koyanagi[1,*]

[1]Laboratory of Viral Pathogenesis, Institute for Virus Research, Kyoto University, Sakyo-ku, Kyoto 606-8507, Japan
[2]Department of Neurology, Neurological Institute, Graduate School of Medical Science, Kyushu University, Higashi-ku, Fukuoka 812-8582, Japan
[3]AIDS Research Center, National Institute of Infectious Diseases, Shinjuku-ku, Tokyo 162-8640, Japan
[4]Department of Immunology, Graduate School of Medicine, University of the Ryukyus, Nishihara, Okinawa 903-0215, Japan
**Corresponding author: Yoshio Koyanagi, ykoyanag@virus.kyoto-u.ac.jp*

We have discovered that an N-terminal deletion mutant of a membrane protein, CD63, (CD63ΔN) blocks entry of CXCR4-using, T-cell tropic human immunodeficiency virus type 1 (X4 HIV-1) by suppressing CXCR4 surface expression. This suppression was observed for CXCR4 but not for CD4, CCR5, CD25, CD71 or other tetraspanin proteins. The suppression of CXCR4 expression on the plasma membrane appeared to be caused by mislocalization of CXCR4 and exclusive transportation of CXCR4 toward intracellular organelles, mainly late endosomes/lysosomes. Our data suggest that CXCR4 trafficking can be modified in terms of its recruitment to the plasma membrane without enhancing the degradation or arresting vesicular transport of CXCR4.

Key words: cell surface expression, CD63, CXCR4, HIV-1, ligand-independent trafficking

Received 30 November 2007, revised and accepted for publication 27 December 2007, uncorrected manuscript published online 30 December 2007, published online 13 February 2008

It has been formerly shown that some cellular factors have the ability to suppress retroviral replication. Restriction factors, such as APOBEC3G and Trim5α, play a significant role in controlling human immunodeficiency virus type 1 (HIV-1) infection (1), and it is predicted that other cellular factors will also influence HIV-1 replication. Innovative approaches should, therefore, bring to light, as-yet untested, antiviral factors. We have previously reported a cDNA-library-expressing lentiviral vector system used to isolate an inhibitor of HIV-1-induced cytopathic effect (CPE) (2).

HIV-1 infects T cells and macrophages that express surface CD4 and chemokine receptors. CXCR4 is a G-protein-coupled chemokine receptor that acts as a receptor for stromal-cell-derived factor 1 (SDF-1) and one of the co-receptors for HIV-1 (3). SDF-1 has been shown to inhibit X4 HIV-1 infection, probably by promoting removal of CXCR4 from the cell surface via ligand-induced endocytosis (4,5). The endocytosis of CXCR4 from the cell surface occurs through clathrin-coated pits, which results from the binding to β-arrestin and perhaps adaptor protein complex-2 (AP-2) (5–7). The ubiquitination of CXCR4 at the plasma membrane has been shown to facilitate a sorting event leading to its lysosome-dependent degradation (8,9). In general, membrane proteins are synthesized in the endoplasmic reticulum (ER) and the folded proteins are transported through the Golgi apparatus, and undergo modification such as glycosylation. At the *trans*-Golgi network (TGN), mature proteins are subsequently sorted and packaged into specific vesicles destined for the plasma membrane or the endosomes. In the case of lysosome-associated proteins (LAMP), there are two alternative routes from the TGN, one to the plasma membrane and the other to the lysosomes (10). However, it is unclear whether or not CXCR4 can be targeted directly from the TGN to the lysosome. In addition, there has not been a report of any molecule that affects trafficking of CXCR4 to the plasma membrane.

CD63 is a membrane protein belonging to the tetraspanin superfamily, consisting of four transmembrane domains (TM1-4) and two extracellular (EC) domains (1–2). It is widely expressed on the surface of many cell types, forming tetraspanin-enriched microdomains (TEMs) on the plasma membrane with other tetraspanin proteins (11). It is also present in secretory vesicles (12,13) and the membranes of the late endosomes and lysosomes (14,15). At the plasma membrane, CD63 is known to interact with molecules such as integrins (16), a tissue inhibitor of metalloproteinase-1 (17) and syntenin-1 (18), and is thought to regulate signal transduction pathways required for cell adhesion, motility and survival. It was also reported that CD63 is involved with endocytosis of its interaction partners such as the β-subunit of H, K-ATPase (HKβ) (19) or membrane-type 1 matrix metalloproteinase (MT1-MMP) (20). However, its physiological role is still not well understood (21–23).

In this study, by using our screening strategy (2), we identified an N-terminal deletion mutant of CD63 that

belongs to a novel class of HIV-1 entry blockers. This CD63 mutant appeared to suppress CXCR4 on the cell surface by changing CXCR4 intracellular trafficking probably after its dispatch from the TGN. In addition, we found that wild-type CD63 also functions to suppress CXCR4 cell surface expression, which may be a physiological function of the protein.

Results

Isolation of gene encoding an anti-HIV-1 protein

Using a bicistronic lentiviral vector, encoding cDNA and a humanized recombinant green fluorescent protein (hrGFP), we generated a human peripheral blood leukocyte (PBL) cDNA library-transduced $CD4^+$ $CXCR4^+$ T-cell line (MT-4) (2). Although most cells were killed after X4 HIV-1 ($HIV\text{-}1_{NL4\text{-}3}$) infection, some $hrGFP^+$ ($cDNA^+$) cells were found to proliferate continuously for more than 30 days post-infection (dpi), from which it was inferred that these cells were transduced with an anti-HIV-1 cDNA. From these cells, we independently isolated two cDNA clones, each containing a 3′ fragment of *cd63* cDNA spanning nucleotide positions 193 or 228 to the 3′ poly-A sequence (Figure S1). These cDNAs (designated clone 12.03 and clone 12.22, respectively) encode a C-terminal fragment of CD63 that contains 156 amino acid residues (amino acid positions 83–238) initiating from the third methionine (Figure S1). We then confirmed that both clone 12.03 cDNA- and clone 12.22 cDNA-transduced MT-4 cells ($hrGFP^+$) were resistant against HIV-induced CPE (data not shown) and found that there is little expression of HIV-1 antigen on these cells after HIV-1 inoculation (Figure 1A). Thus, we isolated cDNAs as a new inhibitor gene of HIV-1-induced CPE.

To reproduce this inhibition via transduction of the *cd63* gene, we next prepared a wild-type *cd63* cDNA (CD63wt)-expressing lentiviral vector, as well as an N-terminal deletion mutant (CD63ΔN)-expressing lentiviral vector (Figure 1B) encoding a C-terminal fragment of CD63 identical to those of the isolated cDNA clones mentioned above (Figure S1). Western blotting analysis using an anti-CD63 monoclonal antibody (mAb), confirmed that CD63ΔN-expressing lentiviral vector and the two originally-isolated cDNA expressed peptides with identical molecular weight (MW) (data not shown). As CD63 has a tyrosine-based lysosomal sorting motif (LSM; amino acid positions 233–238) that binds to AP-2 μ and AP-3 μ subunits (15), we also prepared an LSM-deleted CD63ΔN mutant (designated CD63ΔNL) (Figure 1B). FLAG-tagged wild-type CD63 (FLAGCD63wt), CD63ΔN (FLAGCD63ΔN), or CD63ΔNL (FLAGCD63ΔNL) DNA was transfected into HeLa-derived MAGIC-5 cells ($CXCR4^+$ $CD4^+$ $CCR5^+$), and expression was confirmed by Western blotting using an anti-FLAG mAb. This revealed that these proteins were heavily glycosylated (Figure 1C). Immunofluorescent analysis using these DNA showed that CD63wt and CD63ΔN was predominantly distributed in the perinuclear region and some CD63ΔN were found in intracellular vesicles (Figure 1D). The majority of CD63ΔNL, however, appeared to accumulate at the plasma membrane with some intracellular staining (Figure 1D, third panel).

Inhibition of HIV-1 infection by transduction of cells with CD63 and CD63 mutants

To examine anti-HIV-1 activity of CD63-transduced cells further, we generated ectopic CD63wt- or CD63 mutant-expressing cells using a bicistronic $H2K^k$-expressing lentiviral vector. Transduction of the gene by this lentiviral vector did not substantially affect cell growth (data not shown). We then evaluated anti-HIV activity using an enhanced GFP (EGFP)-expressing X4 HIV-1 (NL-EGFP) (24). Flow cytometric analyses indicated that HIV-1 infection was clearly inhibited in the CD63wt- and CD63 mutant (i.e. CD63ΔN and CD63ΔNL)-transduced cells compared with untransduced or empty vector-transduced cells. In CD63ΔN-transduced cells, in particular, HIV-1 infection was severely inhibited (Figure 1E, fourth panel). However, when we used a pseudotyped HIV-1 (where the HIV-1 envelope protein was replaced with that of amphotropic Moloney murine leukemia virus, MLV), the infectivity reduction was not observed (Figure 1F), suggesting that this inhibition is virus envelope protein dependent.

We confirmed that CD63ΔN was also able to protect transduced cells against wild-type X4 HIV-1 infection. Following X4 $HIV\text{-}1_{NL4\text{-}3}$ infection, enzyme-linked immunosorbent assays (ELISA) revealed that the level of HIV-1 $p24^{gag}$ protein in the culture supernatant of CD63ΔN-transduced MT-4 and MAGIC-5 cells was approximately 100-fold lower than that of either empty vector-transduced or untransduced cells (Figure 1G, left and center panels). However, in the case of CCR5-using HIV-1 (R5 HIV-1; $HIV\text{-}1_{JR\text{-}CSF}$) infection, there was no apparent effect of CD63ΔN on the concentration of $p24^{gag}$ in the culture supernatant (Figure 1G, right panel). These data suggest that replication of X4 HIV-1 was specifically inhibited by CD63ΔN. In addition, the level of newly synthesized X4 HIV-1 cDNA in the CD63ΔN-transduced cells was clearly lower (Figure 1H), suggesting that entry of X4 HIV-1 was inhibited by CD63ΔN. Taken together, these results suggest that ectopic CD63wt and CD63ΔN specifically inhibit X4 HIV-1 entry. Therefore, we hypothesized that expression of the X4 virus-specific co-receptor molecule, CXCR4, might be downregulated by ectopic expression of CD63wt and CD63ΔN.

Suppression of CXCR4 surface expression by CD63- and its mutant transduction

To examine the correlation between levels of CXCR4 surface expression and the transduction efficiency of CD63wt and its mutants, we transduced CD63 into cells in different multiplicity of infection (MOI) using a bicistronic $H2K^k$-expressing lentiviral vector. Flow cytometric analysis using an anti-$H2K^k$ mAb confirmed that higher MOI increased transduction efficiency (data not shown). The flow cytometric analyses using an anti-CXCR4 mAb (A-80)

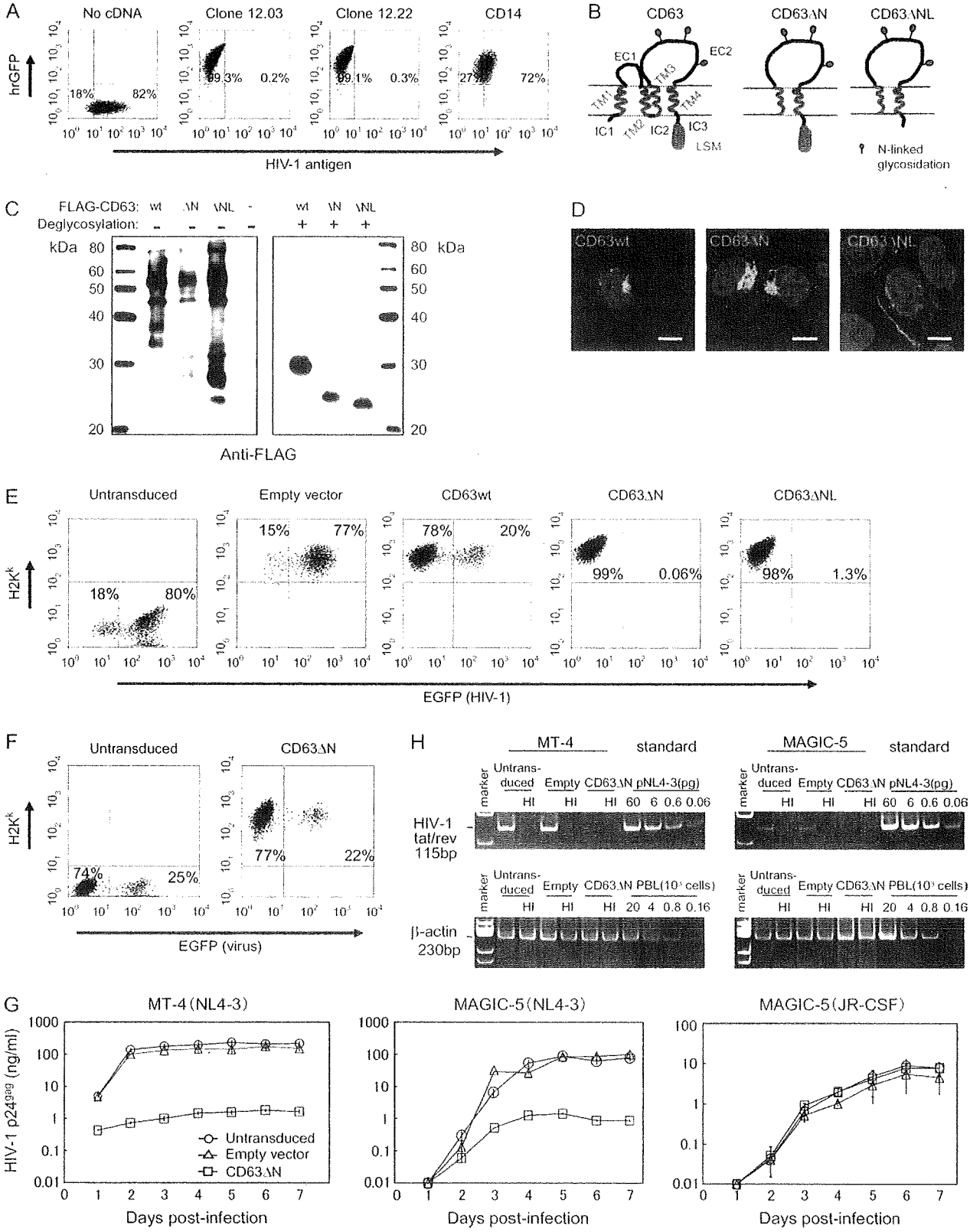

Figure 1: Legend on next page.

indicated that the level of CXCR4 surface expression on CD63wt-transduced MT-4 cells clearly decreased with increased MOI (Figure 2A). A much more obvious suppression of CXCR4 surface expression was found on CD63ΔN-transduced cells (Figure 2A). The suppression of CXCR4 surface expression was further confirmed using another anti-CXCR4 mAb (12G5) (25), which reacts with a different epitope (data not shown). The CD63ΔN-induced suppression of CXCR4 surface expression was only partially impaired by LSM deletion (CD63ΔNL in Figure 2A), and a CD63 mutant lacking LSM (CD63ΔL) still has suppressive activity (data not shown). Suppression of cell surface expression of CXCR4 was also found in 293T cells co-transfected with CXCR4 and CD63ΔN DNA (data not shown).

Suppression of surface expression in CD63wt or CD63 mutant-transduced MT-4 cells was detectable only in CXCR4, but not in CD25 [interleukin (IL)-2 receptor α chain] (Figure 2B), or CD71 (transferrin receptor) molecules (Figure 2C). The suppression of CXCR4, but not CCR5, CD4 or CD71 was also found in CD63ΔN-transduced MAGIC-5 cells (Figure 2D). In addition, the suppression of other tetraspanin proteins such as CD9, CD53, CD81, CD82 and CD151 was not found in CD63ΔN-transduced MAGIC-5 cells (data not shown). Fluorescent microscopic analysis on live cells, using a third anti-CXCR4 mAb (A-145), confirmed the loss of surface CXCR4 on CD63ΔN-transduced MAGIC-5 cells (Figure 2E). Significant suppression was also seen in human $CD4^+$ T cells derived from peripheral blood mononuclear cells (PBMC), which are natural target cells for HIV-1 (Figure 2F). To further confirm the CXCR4 suppression, we assessed the ability of the transduced cells to migrate in response to SDF-1 stimulation. We treated CD63ΔN-transduced MAGIC-5 cells with SDF-1 and found a severe suppression of chemotaxis response in CD63ΔN-transduced cells compared with that of empty vector-transduced cells (Figure 2G). From these results, we concluded that ectopic CD63, especially CD63ΔN, induces significant downregulation of CXCR4 surface expression, because it (i) protects cells against X4 HIV-1 infection, (ii) renders cell surface expression of CXCR4 undetectable when analyzed using 3 anti-CXCR4 mAbs or (iii) renders cells unable to respond to SDF-1.

Involvement of CD63 in regulation of CXCR4 cell surface expression

To clarify whether physiological CD63 plays a role in the regulation of CXCR4 surface expression, we next depleted endogenous CD63 in empty vector-transduced cells using three small interfering RNA (siRNA) oligonucleotides against *cd63*. Immunofluorescent analysis indicated a clear depletion of intracellular CD63 by these siRNAs compared with control siRNA (Figure 3A). Flow cytometric analysis also indicated a significant reduction in CD63 surface expression by these siRNAs (Figure 3B). Levels of CXCR4 surface expression on *cd63*-depleted cells were clearly higher than that on control cells (Figure 3C), indicating that depletion of CD63 resulted in an increased level of CXCR4 surface expression. Combined with the data from CD63wt-transduced cells (Figure 2A), we deduced that CD63 may also negatively regulate CXCR4 surface expression.

Induction of CXCR4 mislocalization by CD63ΔN

To address how CD63ΔN suppresses CXCR4 surface expression, we considered the following possibilities: (i) suppression of CXCR4 mRNA or protein expression;

Figure 1: Specific inhibition of X4 HIV-1 infection by CD63 mutants. A) Little expression of HIV-1 antigen was detected in MT-4 cells transduced with the two putative CD63 C-terminal cDNAs (clone 12.03 and clone 12.22). Four days after HIV-1_{NL4-3} infection, HIV-1 antigen expression on transduced cells was examined using anti-HIV-1 human sera. The level of hrGFP indicates the efficiency of cDNA transduction (*y*-axis). The numbers in each quadrant indicate the percentage of HIV antigen (+) and (−) cells. CD14 is a control having some level of anti-HIV-1 activity as we have previously reported (2). The results of one of three, independently conducted, experiments are shown. B) Structure of CD63 and its mutants. CD63 is comprised of four transmembrane domains (TMs), a small extracellular loop (EC1), a four amino acid intracellular loop (IC2), and a large extracellular loop (EC2), as well as 11 amino acid N-terminal and a 10 amino acids C-terminal tail (containing the LSM). C) CD63 and its mutants are heavily glycosylated. MAGIC-5 cells were transfected with FLAGCD63wt or FLAGCD63-mutant DNA. Cell extracts were incubated in the presence (right panel) or absence (left panel) of deglycosidase and then subjected to Western blot analysis using an anti-FLAG mAb. D) Localization of CD63wt and CD63 mutants. MAGIC-5 cells were transfected with FLAGCD63wt or FLAGCD63-mutant DNA, stained with an anti-FLAG mAb, and analyzed by confocal microscopy. Images were acquired through band-pass filters (BPF) 500–520 nm (FLAG: green) and BPF 420–470 nm (Hoechst; nuclei staining: blue). Scale bars, 10 μm. E) Inhibition of HIV-1 infection by transduction of CD63wt or CD63 mutants. CD63wt-, CD63ΔN-, and CD63ΔNL-transduced MT-4 cells were challenged with NL-EGFP at a MOI of 0.1. Three days after HIV-1 infection, cells were stained with an anti-$H2K^k$mAb, and analyzed by flow cytometry. Surface expression of $H2K^k$gave an indication of transduction efficiency (*y*-axis). The numbers in each quadrant indicate the percentage of EGFP (+) and (−) cells. The results of one of three, independently conducted, experiments are shown. F) No inhibition of MLV Env-pseudotyped HIV-1 infection by transduction of CD63ΔN. CD63ΔN-transduced MT-4 cells were also challenged with an amphotropic MLV Env-pseudotyped EGFP-expressing HIV-1. The numbers in each quadrant indicate the percentage of EGFP (+) and (−) cells. The results of one of three, independently conducted, experiments are shown. G) Lower X4 HIV-1 production in CD63ΔN-transduced cells. The amount of HIV $p24^{gag}$ in cell culture supernatant was followed using ELISA after wild-type HIV-1 infection (left panel: X4 HIV-1_{NL4-3}-infected MT-4 cells; center panel: X4 HIV-1_{NL4-3}-infected MAGIC-5 cells; and right panel: R5 HIV-1_{JR-CSF}-infected MAGIC-5 cells). H) Blocking of X4 HIV-1 entry in CD63ΔN-transduced cells. The level of synthesized HIV-1 cDNA in cells was semiquantified by PCR. HI indicates heat inactivated HIV-1. HIV-1 plasmid DNA was used for marker standards (left: X4 HIV-1_{NL4-3}-infected MT-4 cells; and right: X4 HIV-1_{NL4-3}-infected MAGIC-5 cells). β-actin serves as a control.

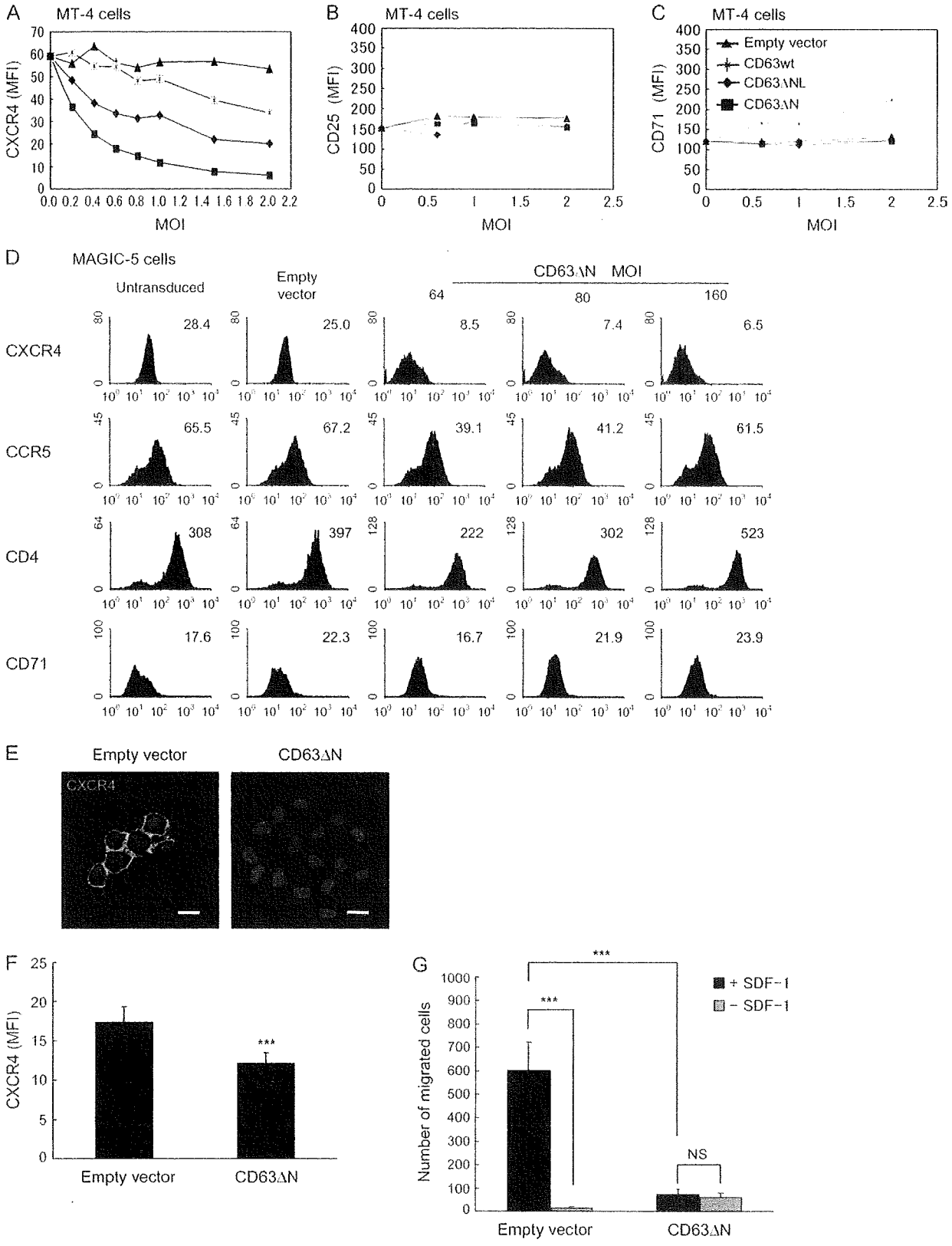

Figure 2: Legend on next page.

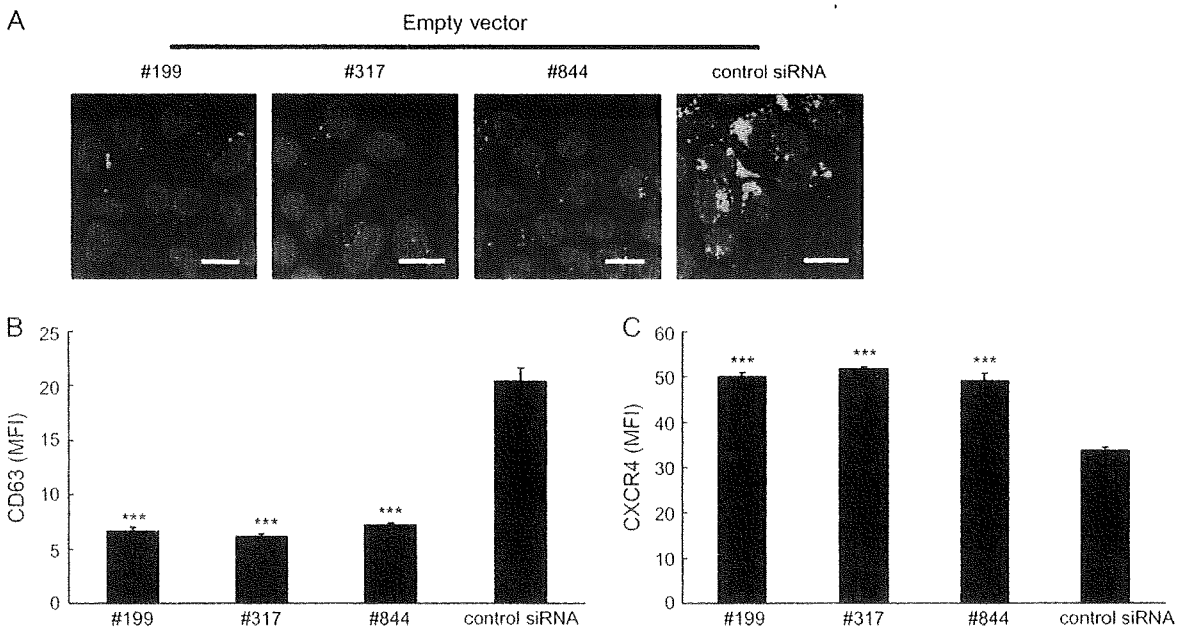

Figure 3: Suppression of CXCR4 surface expression by endogenous CD63. (A) Efficient depletion of endogenous CD63. Empty vector-transduced MAGIC-5 cells were transfected with siRNA oligonucleotides against *cd63* or control siRNA, then stained with an anti-CD63 mAb, and analyzed by confocal microscopy. Images were acquired through band-pass filters (BPF) 500–520 nm (CD63: green) and BPF 420-470 nm (Hoechst: blue). Scale bar, 30 μm. (B, C) Significant reduction of CD63 and augmentation of CXCR4 surface expression on *cd63*-depleted MAGIC-5 cells. CD63 (B) or CXCR4 (C) expression on empty vector-transduced cells treated with siRNA oligonucleotides against *cd63* was measured by flow cytometry. Data are represented as mean ± SED, $n = 3$, $^{***}P < 0.05$ (vs. control siRNA).

(ii) disappearance of CXCR4 protein because of its rapid degradation; or (iii) mislocalization of CXCR4 protein.

Firstly, we compared the amounts of CXCR4 protein in untransduced cells and cells transduced with CD63ΔN or empty vector. Western blotting analysis indicated that the total amounts of CXCR4 protein were very similar in these cells (Figure 4A), suggesting that possibility (i) can be eliminated.

Next, we compared the rate of CXCR4 degradation in empty vector- and CD63ΔN-transduced cells. From examination of CXCR4 expression in cells transfected with pHA-CXCR4 after cycloheximide (CHX) treatment, an inhibitor of translation, we found that the degradation rate of CXCR4 was very similar between empty vector- and CD63ΔN-transduced MAGIC-5 cells (Figure 4B). Under the same condition, we found that little CD63ΔN degradation occurred (data not shown). These data suggest that possibility (ii) can be eliminated.

From immunofluorescent staining, we found that there was a large amount of intracellular CXCR4 in CD63ΔN-transduced cells, while the majority of CXCR4 localized at the plasma membrane in untransduced or empty vector-transduced cells (Figure 4C). To confirm this phenomenon, we next transfected an hrGFP-tagged CXCR4 DNA (phrGFPCXCR4) into empty vector- or CD63ΔN-transduced MAGIC-5 cells. This enabled us to visualize the location of CXCR4 molecules in live cells. CXCR4 was predominantly

Figure 2: Suppression of CXCR4 surface expression by CD63 or CD63 mutants. A–C) The surface expression of CXCR4 (A), CD25 (B) or CD71 (C) on CD63wt- or CD63 mutant-transduced MT-4 cells was measured by flow cytometry. The *x*-axis indicates MOI of lentiviral vector and *y*-axis indicates the mean fluorescence intensity (MFI). A-80 mAb was used for CXCR4-staining. D) Surface expression of CXCR4, CCR5, CD4 or CD71 on CD63ΔN-transduced MAGIC-5 cells was measured by flow cytometry. The number in each panel indicates the MFI of each molecule. E) The disappearance of CXCR4 on the cell surface of CD63ΔN-transduced MAGIC-5 cells. Empty vector- or CD63ΔN-transduced cells were incubated with another anti-CXCR4 mAb (A-145) at 4°C without permeabilization and analyzed by confocal microscopy. Images were acquired through band-pass filters (BPF) 500–520 nm (CXCR4: green) and BPF 420–470 nm (Hoechst: blue). Scale bars, 20 μm. F) Surface expression of CXCR4 on the CD63ΔN-transduced human $CD4^+$ T cells derived from PBMC. Six days after transduction, cells were stained with an anti-CXCR4 mAb (A-80) and analyzed. MFI of CXCR4 is shown. Data are represented as mean ± SED, $n = 4$, $^{***}P < 0.05$ (vs. empty vector). G) Chemotactic response of MAGIC-5 cells to SDF-1 was reduced by transduction of CD63ΔN. Cells were cultured in the presence (black filled) or absence (grey filled) of SDF-1. Chemokine-mediated migration of cells is expressed as the mean number of migrated cells per three examined fields. Data are represented as mean ± SED, $n = 3$, $^{***}P < 0.05$, NS, not significant.

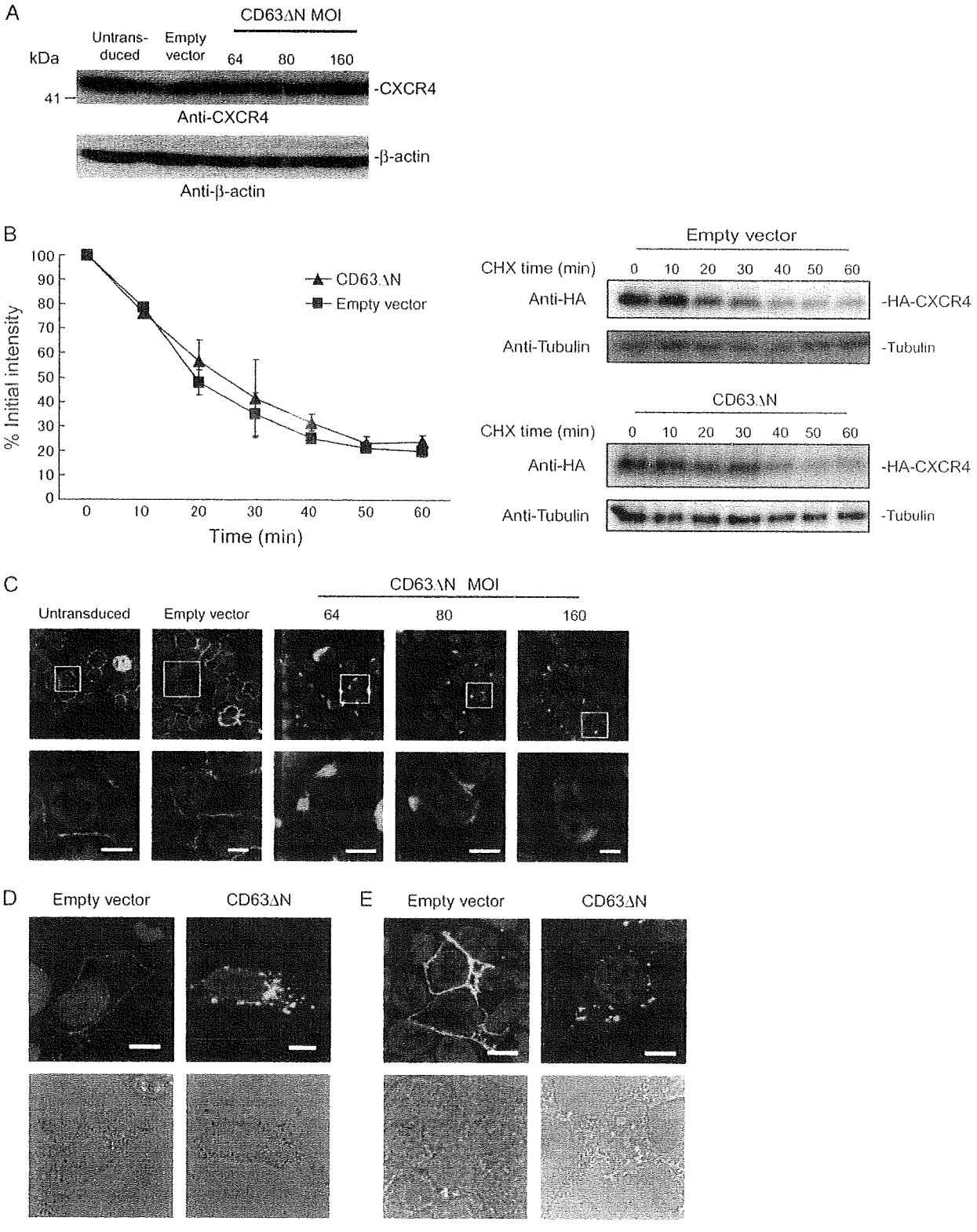

Figure 4: Legend on next page.

localized at the plasma membrane in empty vector-transduced cells, while large amounts of intracellular CXCR4 was found in CD63ΔN-transduced cells (Figure 4D). Intracellular CXCR4 was also found in 293T cells co-transfected with CD63ΔN DNA and phrGFPCXCR4 (Figure 4E). These data strongly suggest that CD63ΔN induces the mislocalization of CXCR4, in which localization of CXCR4 was shifted from the plasma membrane to intracellular membrane.

The mislocalization of CXCR4 might not be due to dynamin-dependent internalization

To clarify the mechanism of this mislocalization, we hypothesized that in CD63ΔN-transduced cells, (i) endocytosis of CXCR4 from the cell surface is strongly augmented; (ii) the intracellular trafficking of CXCR4 via vesicular transport is inhibited or (iii) CXCR4 is transported only to intracellular organelles. To examine CXCR4 surface expression on live cells over a set period of time, we cultured empty vector- or CD63ΔN-transduced MAGIC-5 cells in the presence of an fluorescein isothiocyanate (FITC)-conjugated anti-CXCR4 mAb and then assessed CXCR4 surface expression using confocal microscopy (Figure 5A). Thirty minutes after initiation of culture, CXCR4 was detected on the plasma membrane of empty vector-transduced cells (Figure 5A,c) but not visible on CD63ΔN-transduced cells (Figure 5A,e). Small green spots, probably unspecifically endocytosed or pinocytosed mAb, were also detected not only in cells cultured with anti-CXCR4 mAbs (Figure 5A,c.e) but also in cells cultured with an FITC-conjugated control immunoglobulin (Ig) G (Figure 5A,a). We next carried out the similar experiment in the presence of an actin polymerization inhibitor, cytochalasin D, and confirmed that there was little captured control IgG (Figure 5A,g). In this condition, CXCR4 on the plasma membrane was detected only in empty vector-transduced cells (Figure 5A,i), but not visible in CD63ΔN-transduced cells (Figure 5A,k). CXCR4 on the cell surface was not detected in CD63ΔN-transduced cells after further incubation (120 min) (Figure 5A,o). In addition, we transfected a dominant negative mutant of dynamin 1 (Dynamin 1 K44A) DNA into CD63ΔN-transduced MAGIC-5 cells to block dynamin-dependent CXCR4 internalization (7,8). Although we found the accumulation of transferrin receptor (CD71) on the cells after transfection with Dynamin 1 K44A DNA, we could not observe any recovery of CXCR4 surface expression in the cells (Figure 5B). These data suggest that the CD63ΔN-induced CXCR4 mislocalization might not be the result of dynamin-dependent internalization.

Intracellular trafficking of CXCR4 via transport vesicles is not inhibited in CD63ΔN-transduced cells

To examine the longitudinal distribution of CXCR4 molecules in live cells, we prepared a haloalkane dehalogenase-tagged (Halo-tagged) CXCR4 DNA (pHalo-CXCR4) and transfected it into empty vector- or CD63ΔN-transduced MAGIC-5 cells. After staining with HaloTag^{TM}-specific labeling ligand (Halo-ligand), we found that CXCR4 was localized predominantly at the plasma membrane and partly in the intracellular compartment including ceramide^{+} Golgi apparatus of empty vector-transduced cells (Figure 6A, upper left panel). The labeled CXCR4 at the plasma membrane was rapidly internalized after SDF-1 stimulation (data not shown), indicating that Halo-tagged CXCR4 represents natural CXCR4 distribution. In CD63ΔN-transduced cells, however, we detected most CXCR4 in the intracellular membrane containing the ceramide^{+} Golgi apparatus, but not at the plasma membrane (Figure 6A, upper center panel). In addition, we observed many vesicle-like CXCR4^{+} ceramide^{-} spots in the cytoplasm of these cells (arrow heads in Figure 6A upper center panel). To confirm rigidly that the signal of these spots reflected the existence of Halo-tagged CXCR4, we treated transfected cells with Brefeldin A (BFA), an inhibitor of vesicle transport from the ER to the Golgi apparatus. We detected only reticulated distribution of CXCR4 but no vesicle-like spots in the treated cells (Figure 6A, right panel), confirming that these spots were CXCR4-containing vesicles. The longitudinal distribution of CXCR4 was next traced over 30-min time intervals (Figure 6B,C). Although we detected many CXCR4-containing vesicles during observation (arrow heads in Figure 6C), no CXCR4 at the plasma membrane was found in CD63ΔN-transduced cells. To further examine CXCR4-containing vesicles in detail, we performed analyses using total internal reflection fluorescence microscopy (TIRFM). This microscopy is adequate to trace vesicles within approximately 150 nm of the plasma membrane (adhered surface). We transfected CXCR4EGFP into empty vector- or CD63ΔN-transduced MAGIC-5 cells and successfully detected many CXCR4-containing vesicles (Figure 6D,E, upper left panels). We found a similar

Figure 4: Induction of CXCR4 mislocalization by CD63ΔN. A) Total CXCR4 expression is similar independent of CD63ΔN-transduction in MAGIC-5 cells. The total amounts of CXCR4 protein in empty vector- or CD63ΔN-transduced cells was measured by Western blotting using an anti-CXCR4 mAb (A-145). β-actin serves as a control. B) The degradation rate of HA-tagged CXCR4 in empty vector- or CD63ΔN-transduced MAGIC-5 cells. The degradation of CXCR4 in the presence of CHX was assessed by Western blotting. The decay graph shows average of three independent trials (right panel). The images of one representative blot are also shown. Tubulin serves as a control. C) Intracellular CXCR4 was found in CD63ΔN-transduced MAGIC-5 cells. Cells were stained with an anti-CXCR4 mAb (A-145), and analyzed by confocal microscopy. Images were acquired through BPF 500–520 nm (CXCR4: green) and BPF 420–470 nm (Hoechst: blue). Scale bars, 10 μm. D, E) Intracellular CXCR4 was detected in the presence of CD63ΔN. Empty vector- or CD63ΔN-transduced MAGIC-5 cells transfected with phrGFPCXCR4 (D), and 293T cells co-transfected with phrGFPCXCR4 and empty vector or CD63ΔN DNA (E), were analyzed by confocal microscopy. Images were acquired through band-pass filters (BPF) 500–520 nm (GFP: green) and BPF 420–470 nm (Hoechst: blue). Scale bars, 10 μm. DIC images are also shown (lower panel).